

Highlights from the STAR experiment

Hanna Zbroszczyk

for the STAR Collaboration

Faculty of Physics, Warsaw University of Technology

supported by National Science Centre, Poland

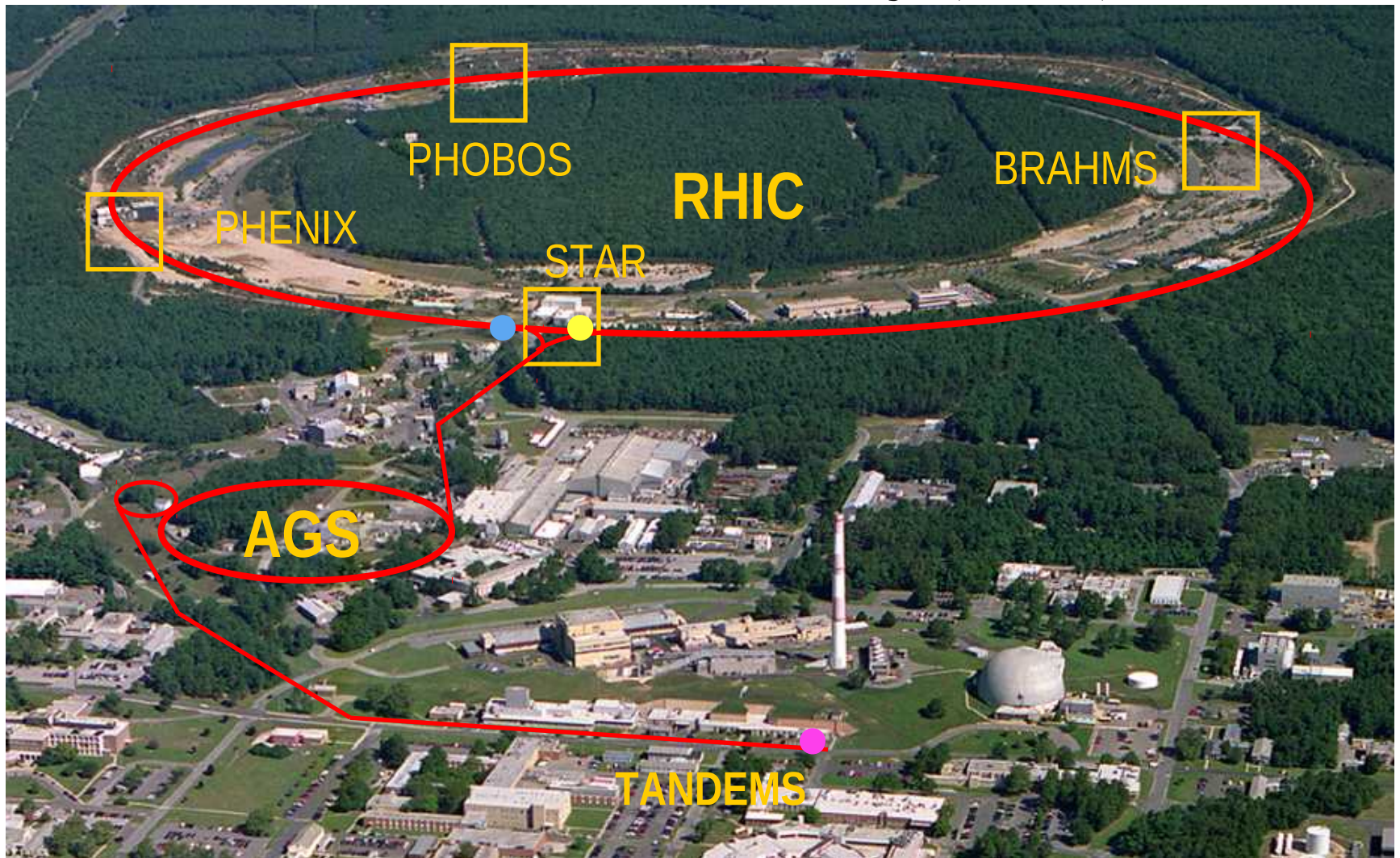




Introduction

Relativistic Heavy Ion Collider (RHIC)

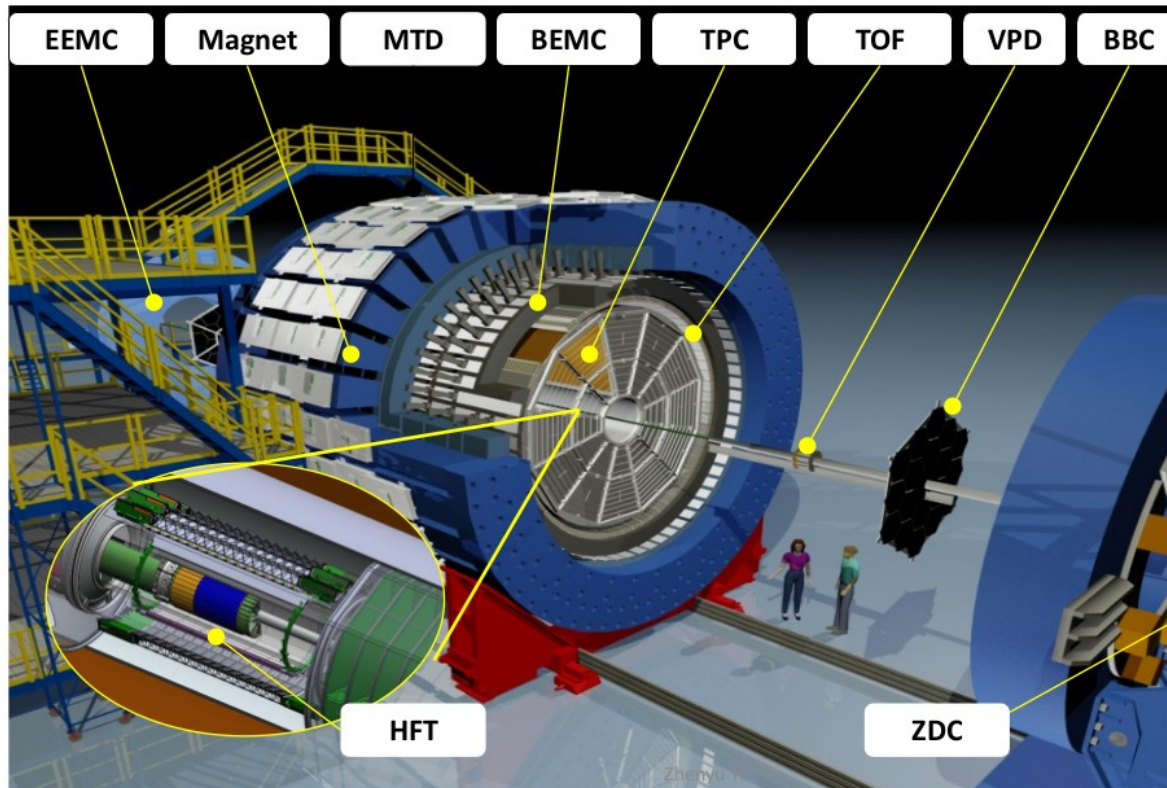
Brookhaven National Laboratory (BNL), New York



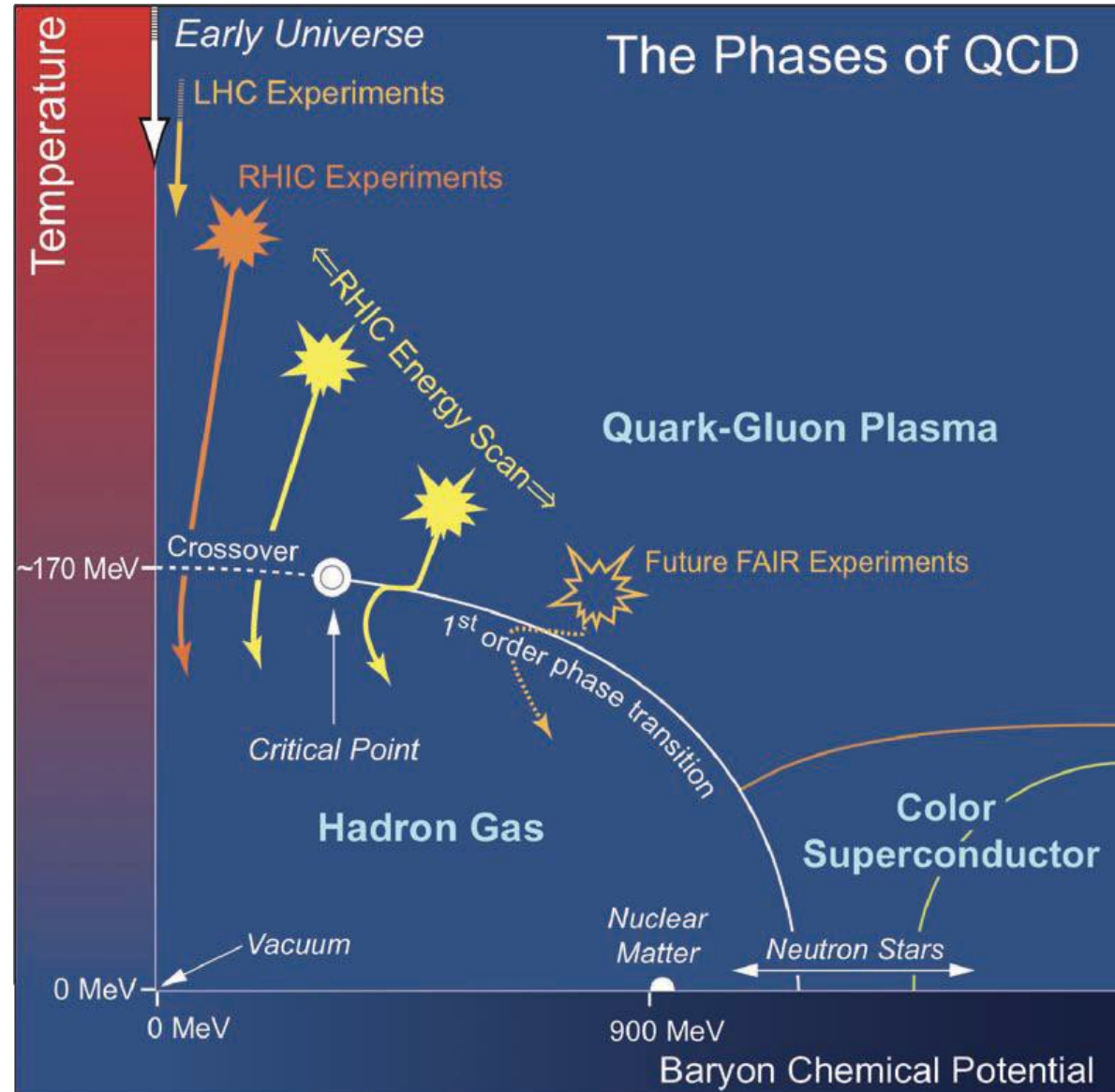
- 2 concentric rings of 1740 superconducting magnets
- 3.8 km circumference

The Solenoidal Tracker At RHIC

- **Tracking and PID (full 2π)**
 - TPC: $|\eta| < 1$
 - TOF: $|\eta| < 1$
 - BEMC: $|\eta| < 1$
 - EEMC: $1 < \eta < 2$
 - HFT (2014-2016): $|\eta| < 1$
 - MTD (2014+): $|\eta| < 0.5$
- **MB trigger and event plane reconstruction**
 - BBC: $3.3 < |\eta| < 5$
 - EPD (2018+): $2.1 < |\eta| < 5.1$
 - FMS: $2.5 < \eta < 4$
 - VPD: $4.2 < |\eta| < 5.1$
 - ZDC: $6.5 < |\eta| < 7.5$
- **On-going/future upgrades**
 - iTPC (2019+): $|\eta| < 1.5$
 - eTOF (2019+): $-1.6 < \eta < -1$



Introduction



RHIC Top Energy

p+p, p+Al, p+Au, d+Au, $^3\text{He}+\text{Au}$, Cu+Cu, Cu+Au, Ru+Ru, Zr+Zr, Au+Au, U+U
QCD at high energy density/temperature
Properties of QGP, EoS

Beam Energy Scan

Au+Au 7.7-62 GeV
QCD phase transition
Search for critical point
Turn-off of QGP signatures

Fixed-Target Program

Au+Au = 3.0-7.7 GeV
High baryon density regime
with 420-720 MeV

Introduction

1. Open heavy flavor - $D^0 v_1$, $D^0 R_{AA}$ and R_{CP} , Λ_C
2. Quarkonium - ΥR_{AA}
3. Jet modification and high- p_T hadrons - di-jet imbalance, di-hadron correlation
4. Chirality, vorticity and polarization effects - Λ polarization, Φ polarization, CME, CMW
5. Initial state physics and approach to equilibrium - v_2 and v_3 fluctuations
6. Collectivity in small systems - v_2 in p+Au and d+Au
7. Collective dynamics - longitudinal decorrelation, identified particle v_1
8. High baryon density and astrophysics - v_1 from fixed target
9. Correlations and fluctuations – femtoscopy
10. Phase diagram and search for the critical point - net Λ and off-diagonal cumulants
11. Thermodynamics and hadron chemistry - triton, hypertriton mass
12. Upgrades - BES-II and forward upgrades

Introduction

1. **Open heavy flavor - $D^0 v_1$, $D^0 R_{AA}$ and R_{CP} , Λ_C**

2. Quarkonium – ΥR_{AA}

3. Jet modification and high- p_T hadrons - di-jet imbalance, di-hadron correlation

4. Chirality, vorticity and polarization effects - Λ polarization, Φ polarization, CME, CMW

2. **Initial state physics and approach to equilibrium - v_2 and v_3 fluctuations**

6. Collectivity in small systems - v_2 in p+Au and d+Au

7. Collective dynamics - longitudinal decorrelation, identified particle v_1

3. **High baryon density and astrophysics - v_1 from fixed target**

4. **Correlations and fluctuations – femtoscopy**

10. Phase diagram and search for the critical point - net Λ and off-diagonal cumulants

5. **Thermodynamics and hadron chemistry - triton, hypertriton mass**

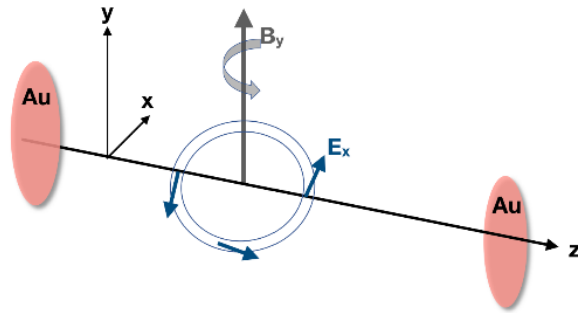
6. **Upgrades - BES-II and forward upgrades (as summary)**



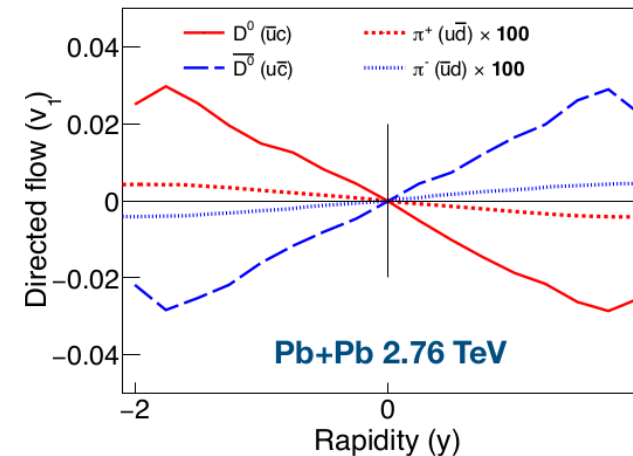
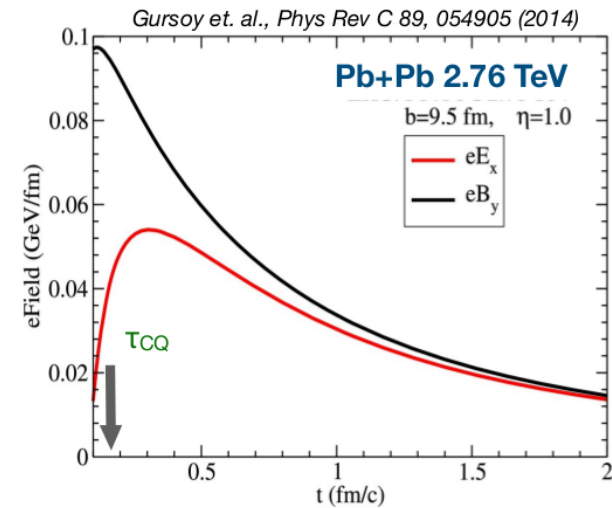


Results

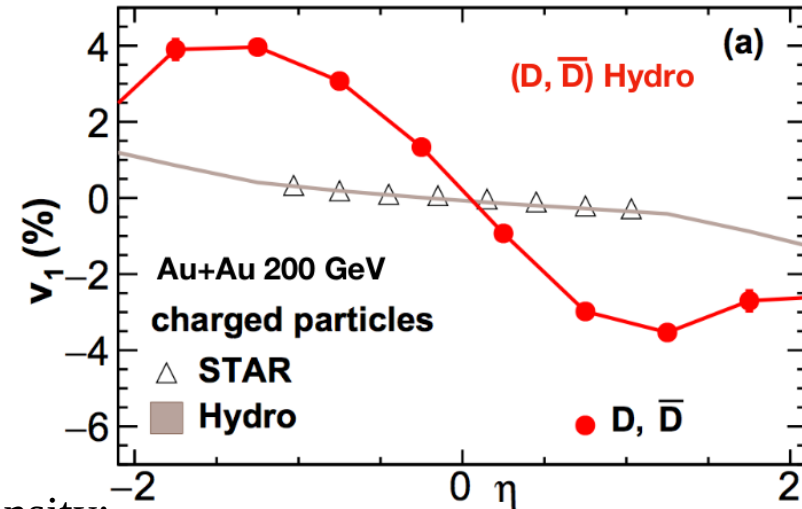
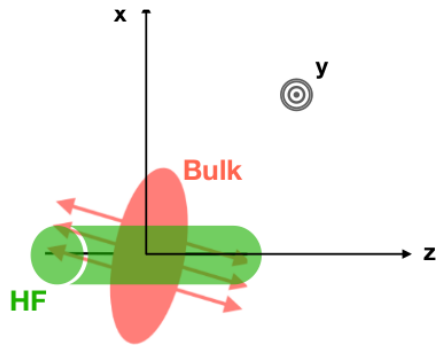
1) D^0 – Open heavy flavor



- The moving **spectators** can produce enormously large **electromagnetic field** ($eB \sim 10^{18}$ G at RHIC)
- Due to **early** production of heavy quarks ($\tau_{CQ} \sim 0.1$ fm/c) positive and negative charm quarks (CQs) can get **deflected** by the initial EM force
- Model predicts **opposite** v_1 for charm and anti-charm quarks induced by this initial EM field
- This induced v_1 depends on the balance between E and B fields
- The **magnitude** of such induced v_1 for heavy quarks is much **larger** than the light quarks



1) D^0 – Open heavy flavor



Chatterjee, Bozek: *Phys Rev Lett* 120, 192301 (2018)

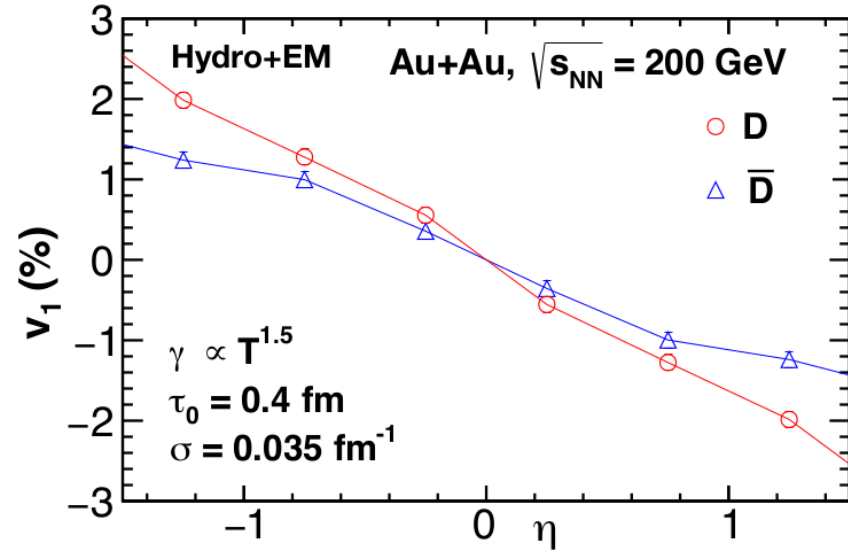
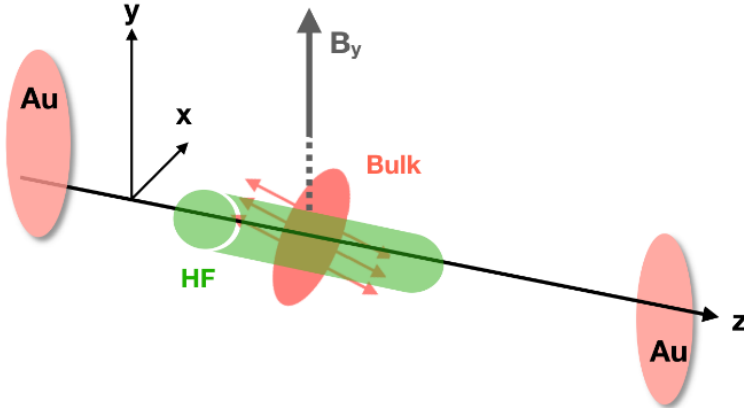
- Heavy quarks are produced according to N_{coll} density: symmetric in rapidity at non-zero rapidity, charm quarks production points are **shifted** from the bulk
- This can induce **larger** v_1 in charm quarks than light flavors
- Magnitude of charm quark v_1 depends on the drag parameter used in this model
- We can probe the longitudinal profile of the initial matter distribution through heavy flavor v_1

(v_1 -slope) Charm-Quark \gg (v_1 -slope) Light-Quark

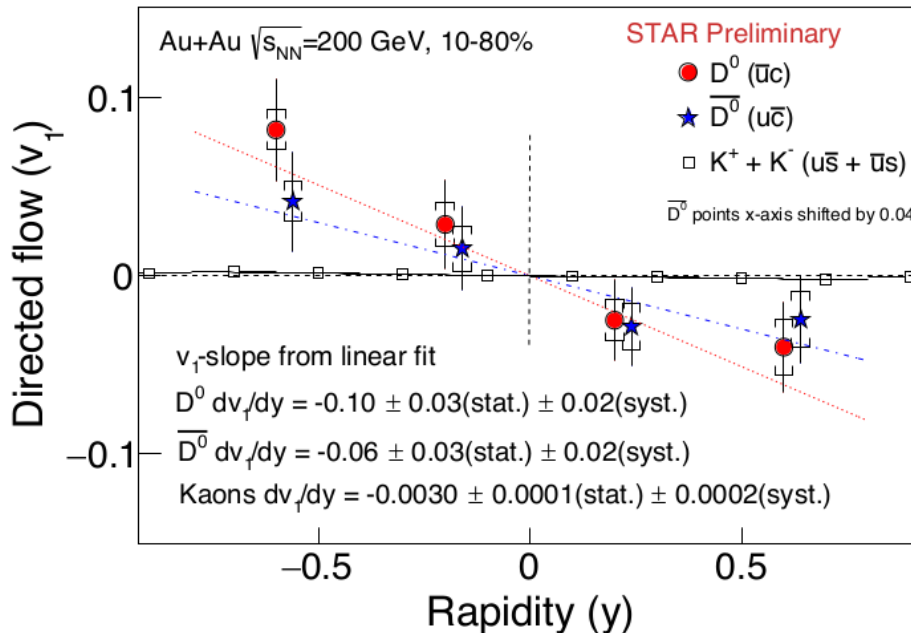
- Charm quarks much more sensitive to the initial tilt than the charged hadrons D^0 (\bar{D}^0) v_1 can be used to constrain drag coefficients in conjunction with v_2 and R_{AA}

1) D^0 – Open heavy flavor

Interplay between the drag by tilted bulk and the EM field



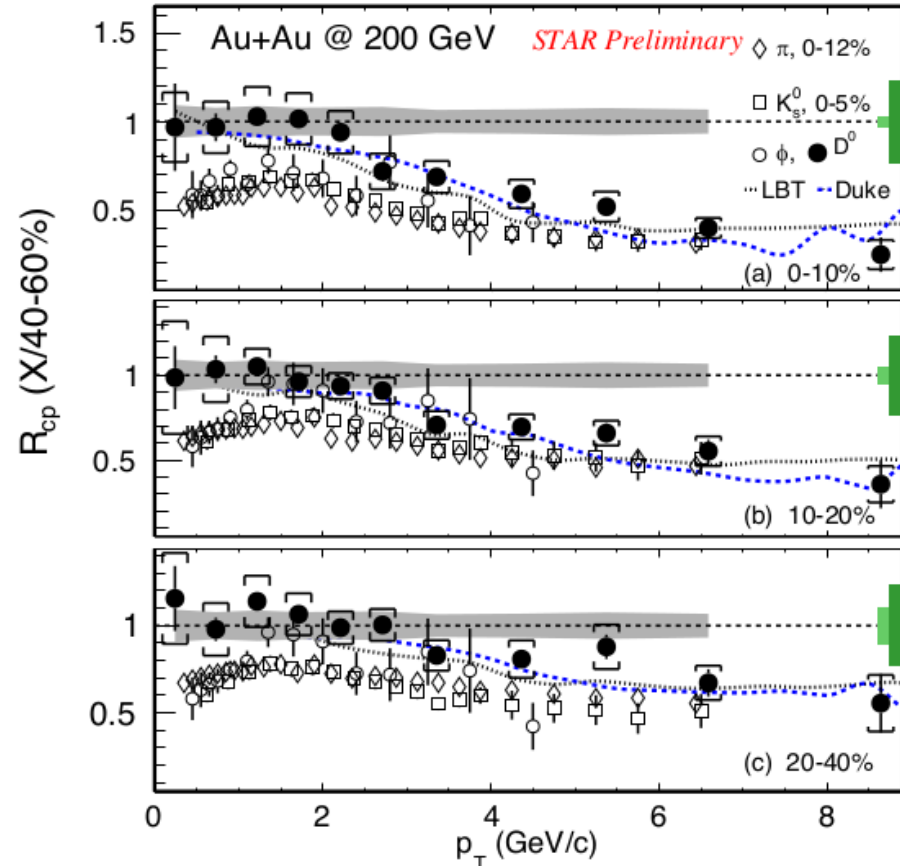
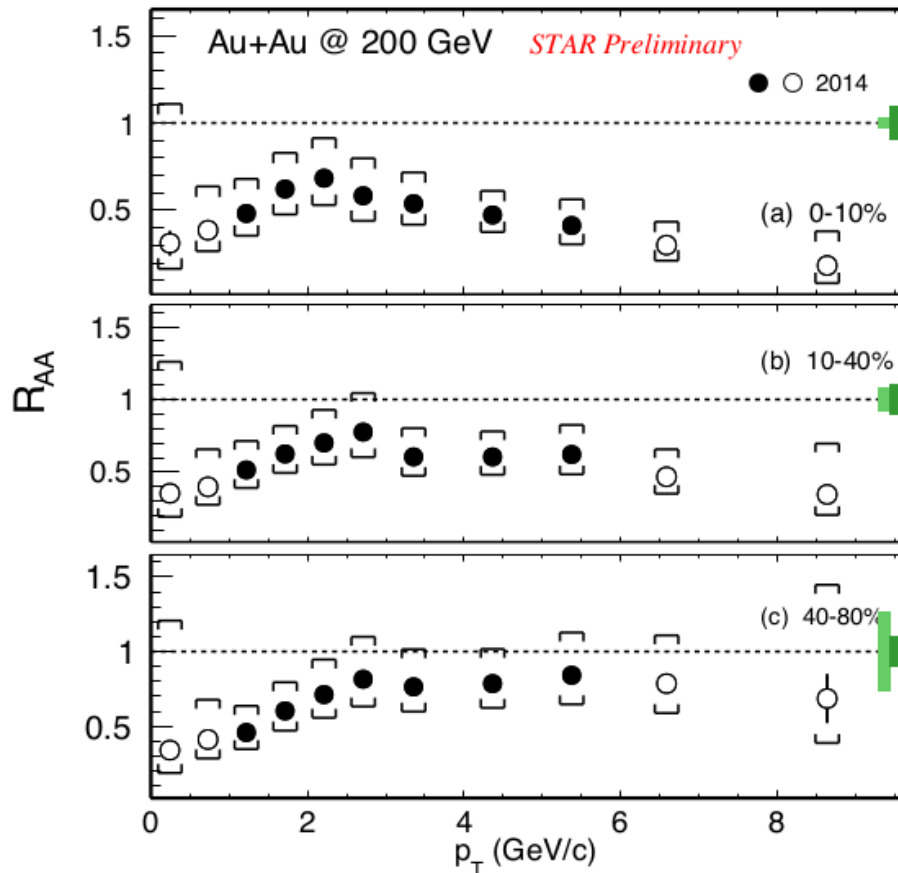
Chatterjee, Bozek: 1804.04893v1



Recent hydro model with initial EM field predicts v_1 **-split** between the D and anti-D meson

D meson v_1 **greater** than the anti-D
 Predicted difference in v_1 is about 10 times smaller than the average v_1

1) D^0 – Open heavy flavor



Significant suppression at **low** p_T with no strong centrality dependence,
 Suppression at **high** p_T decreases towards more peripheral collisions.

Non-prompt D^0 R_{AA} study has been performed, need better precision
 measurements to understand mass dependence of energy loss.

STAR data was re-analysed due to error found during analysis
 → **erratum** will be published soon

1) D^0 – Open heavy flavor

First evidence of non-zero directed flow for heavy flavor

Both D^0 and D^0 show **negative** v_1 -slope near mid-rapidity

Heavy flavor $v_1 >$ light flavor v_1

Data can be used to probe **initial** matter distribution

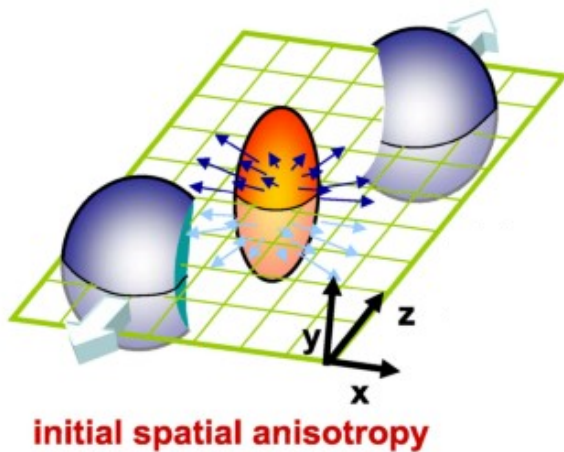
Current precision is **not sufficient** to draw conclusion on
magnetic field induced charge separation of heavy quarks

Non-prompt D^0 R_{AA} study has been performed, need better precision
measurements to understand mass dependence of energy loss.

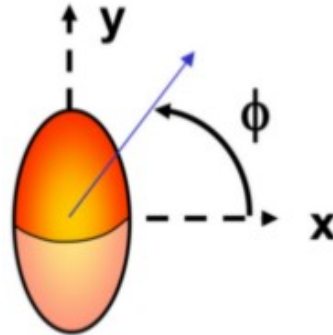
2) Initial state physics

Anisotropic flow in non-central collisions

$$\phi = \text{atan} \frac{p_y}{p_x}$$



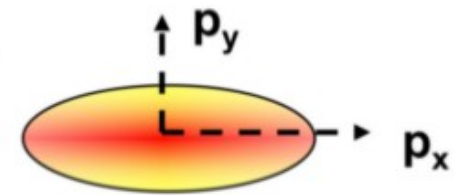
Initial spatial deformation



Rescatterings
(pressure gradients)



Final momentum anisotropy



anisotropy in momentum space

$$E \frac{d^3 N}{dp^3} = \frac{1}{2\pi} \frac{d^2 N}{p_T dp_T dy} \left(1 + 2 \sum_{n=1}^{\infty} v_n \cos [n(\phi - \Phi_R)] \right)$$

2) Initial state physics

Q-cumulant method (traditional)

$$\langle 2 \rangle_n = \langle e^{in(\phi_1 - \phi_2)} \rangle$$

$$v_n^4\{4\} = \langle 4 \rangle_{nn} - 2 \langle 2 \rangle_n \langle 2 \rangle_n$$

$$\langle 4 \rangle_{nm} = \langle e^{in(\phi_1 - \phi_2) + im(\phi_3 - \phi_4)} \rangle$$

$$NSC(n, m) = \frac{\langle 4 \rangle_{nm} - \langle 2 \rangle_n \langle 2 \rangle_m}{\langle 2 \rangle_n^{Sub} \langle 2 \rangle_m^{Sub}}$$

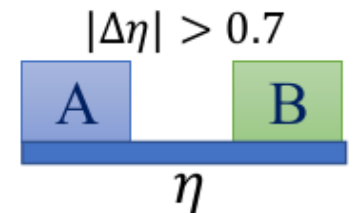
Φ - azimuthal angle

Two-subevent method

$$\langle 2 \rangle_n^{Sub} = \langle e^{in(\phi_A - \phi_B)} \rangle$$

$$v_n^2\{2\} = c_n\{2\} = \langle 2 \rangle_n^{Sub}$$

✓ Short-range non-flow contribution in $v_2\{2\}$ is suppressed by $|\Delta\eta| > 0.7$

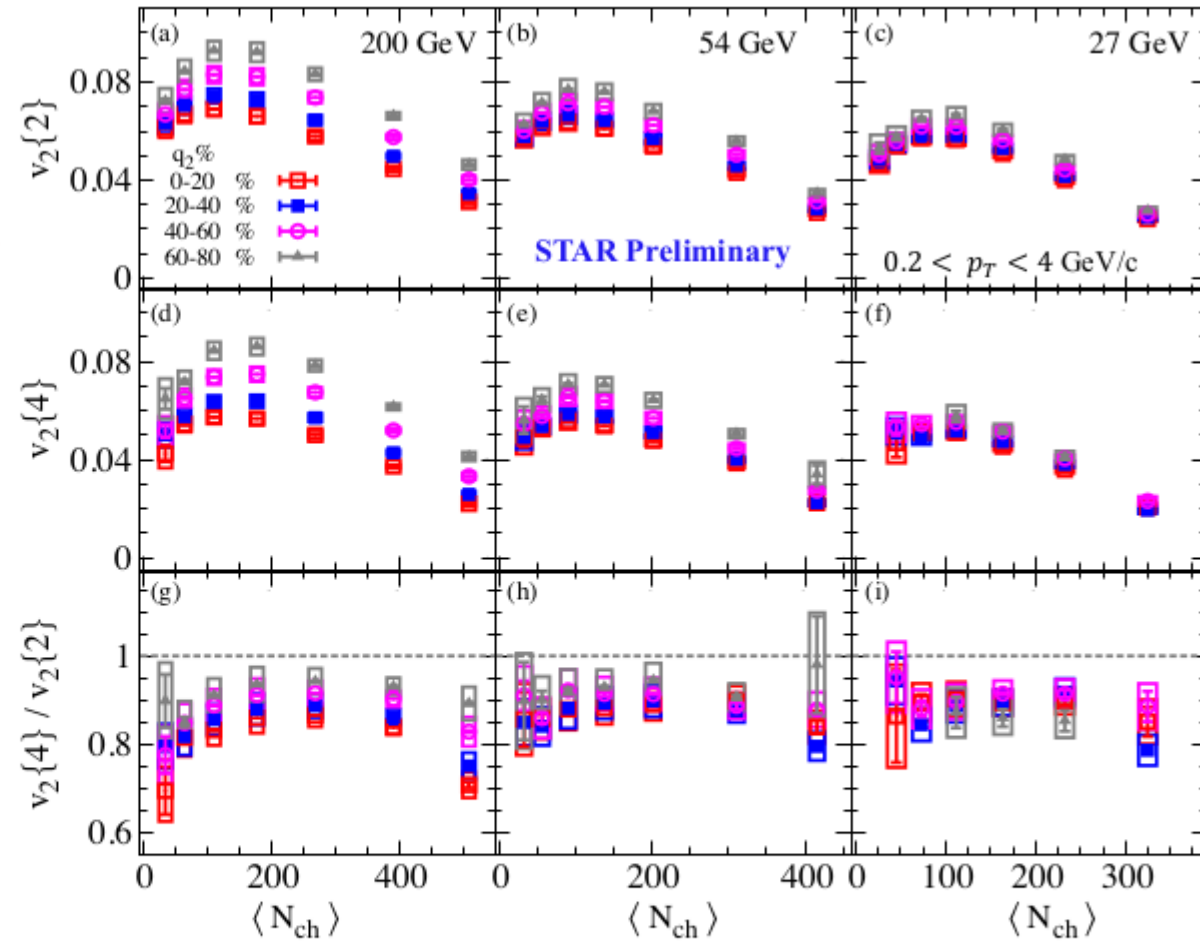


$$v_n^4\{4\} = 2 \langle v_n^2 \rangle^2 - \langle v_n^4 \rangle$$

$$\left[\frac{v_n\{4\}}{v_n\{2\}} \right]^4 = 2 - \frac{\langle v_n^4 \rangle}{\langle v_n^2 \rangle^2}$$

Sensitive to flow fluctuations

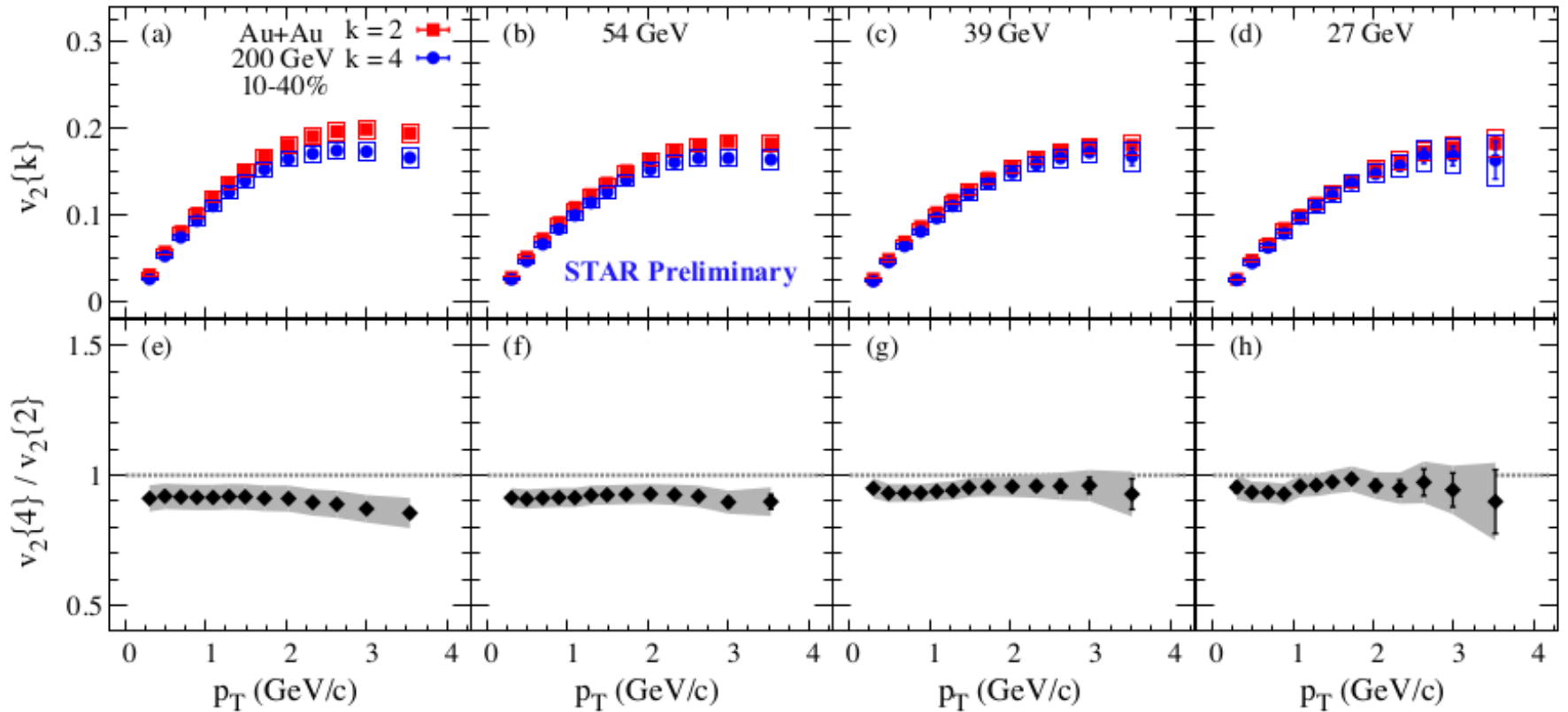
2) Initial state physics



Strong dependence of $v_2\{2\}$ and $v_2\{4\}$ on collision centrality more significant for higher collision energies

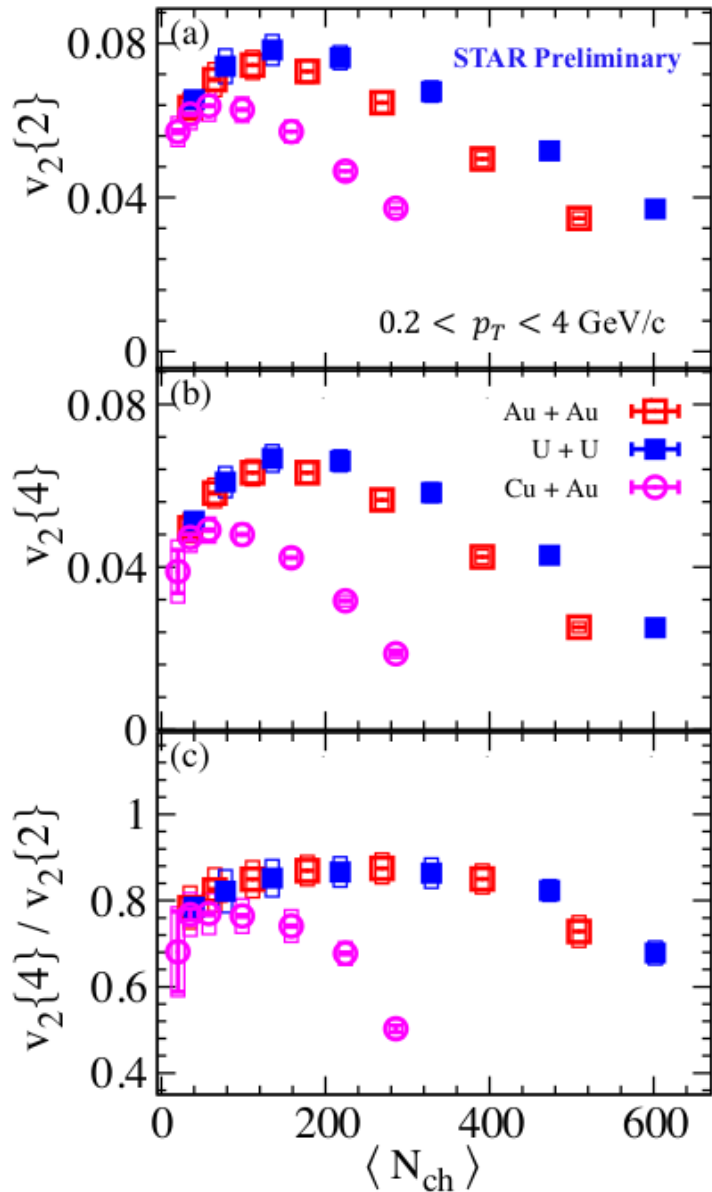
Weak dependence of $v_2\{2\}/v_2\{4\}$ on collision centrality

2) Initial state physics



Weak dependence of $v_2\{2\}$, $v_2\{4\}$ and $v_2\{2\}/v_2\{4\}$
on transverse momentum

2) Initial state physics

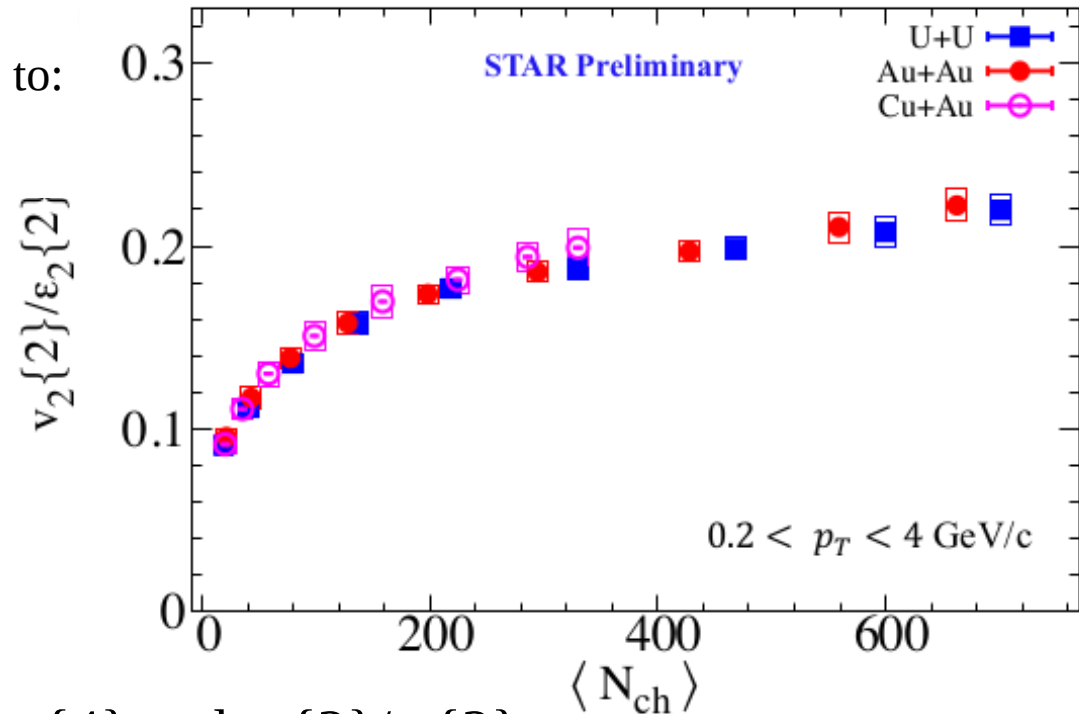


Significant dependence of $v_2\{2\}$, $v_2\{4\}$ and $v_2\{2\}/v_2\{4\}$ on collision centrality for different A+A collisions

2) Initial state physics

Anisotropic flow magnitude is sensitive to:

- initial-state spatial anisotropy
- flow fluctuations and correlations
- viscous attenuation ($\propto \eta/s(T)$)



Weak dependence of $v_2\{2\}$, $v_2\{4\}$ and $v_2\{2\}/\epsilon_2\{2\}$ on collision centrality for various systems.

Are dynamical final-state fluctuations significantly less than the initial-state fluctuations?

2) Initial state physics

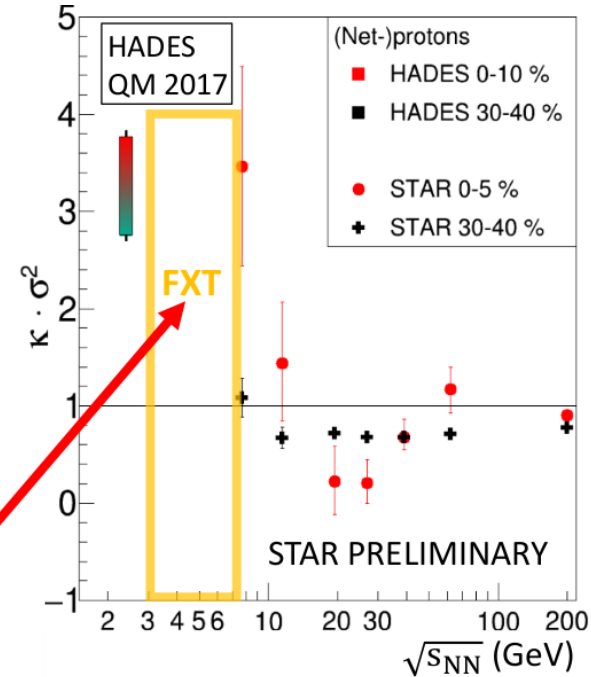
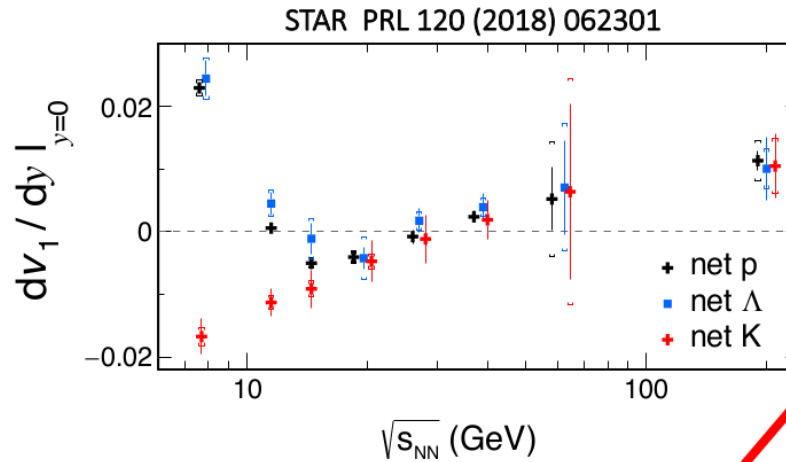
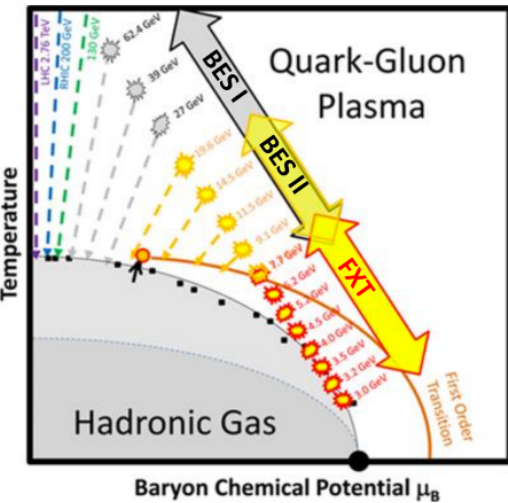
Strong dependence of $v_2\{2\}$, $v_2\{4\}$ on collision centrality, collision energy, transverse momentum

Weak dependence of $v_2\{4\}/v_2\{2\}$ and $v_2\{2\}/\varepsilon_2\{2\}$ (elliptic flow fluctuations) on the size of colliding system and: collision centrality, collision energy, transverse momentum

Flow fluctuations are dominated by the fluctuations of the **initial state eccentricity**

Similar viscous coefficient for different colliding systems

3) Fixed target mode

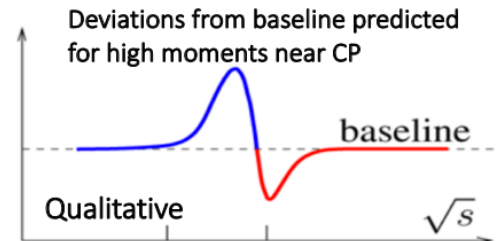


BES goals:

- Search for 1st order phase transition
- Search for existence of the Critical Point
- Search for turn-off QGP signatures

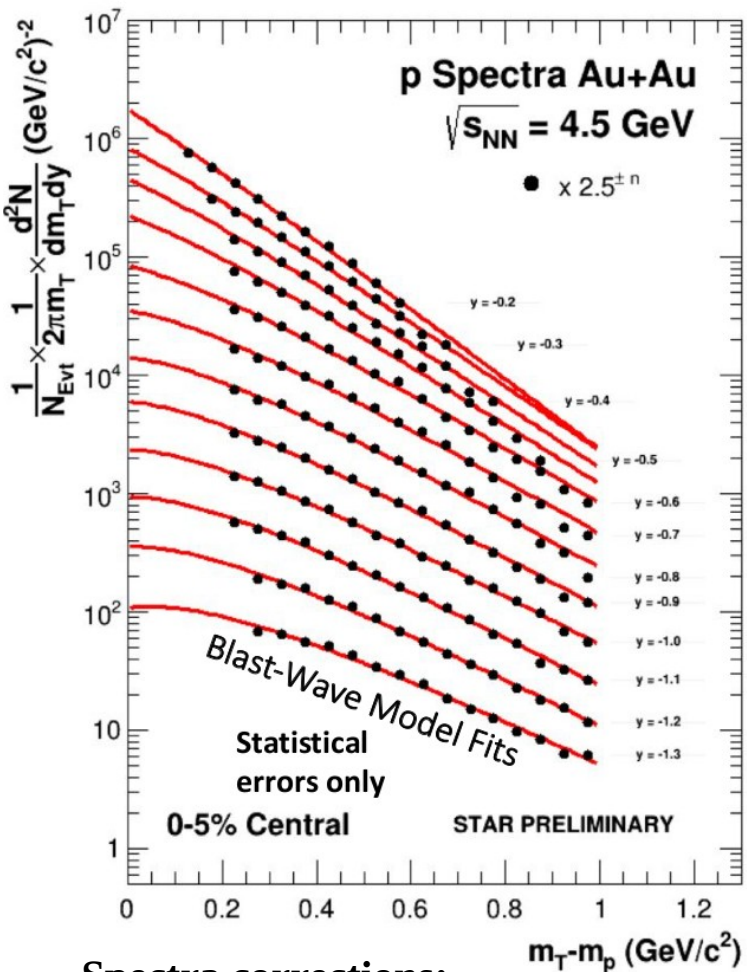
Collider mode is unusable for $\sqrt{s_{NN}} < 7.7$ GeV

Fix target mode is able to cover $\sqrt{s_{NN}}$ from 3.0 GeV to 7.7 GeV



I. Stephanov J Phys G: Nucl Part Phys 38 (2011) 124147

3) Fixed target mode



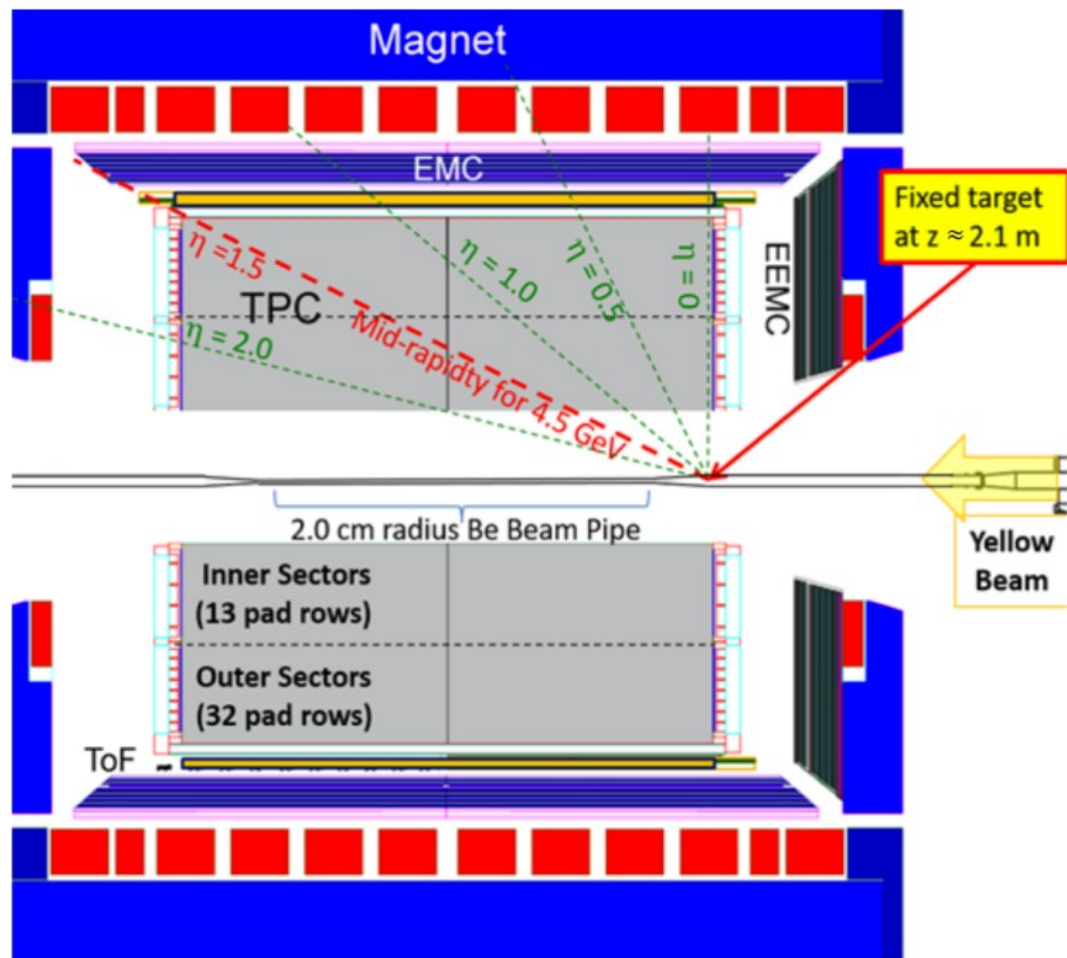
Spectra corrections:

Detector efficiency

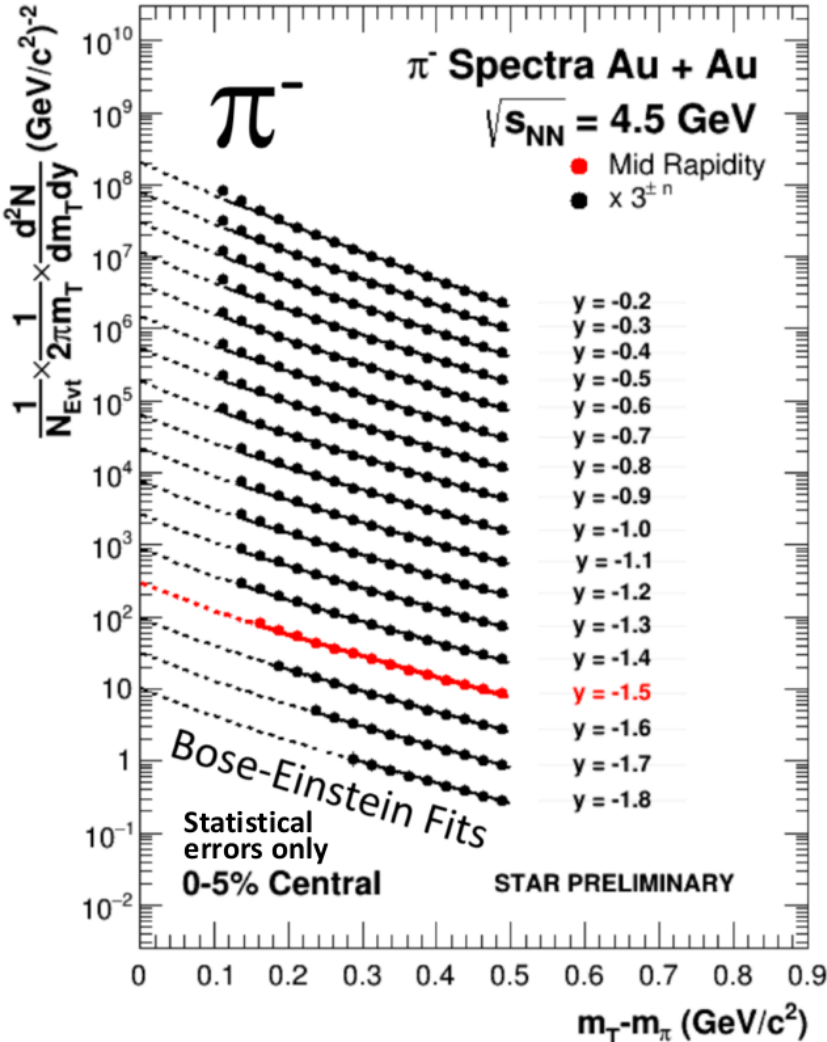
Detector acceptance

(each rapidity window)

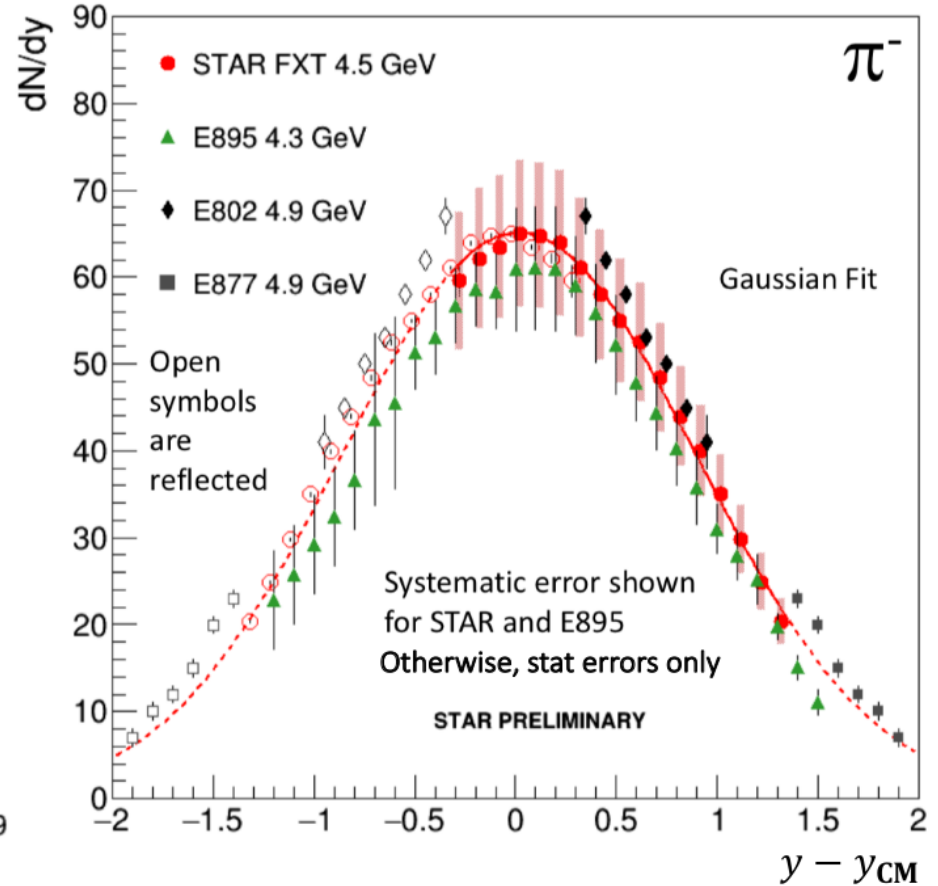
Energy loss



3) Fixed target mode

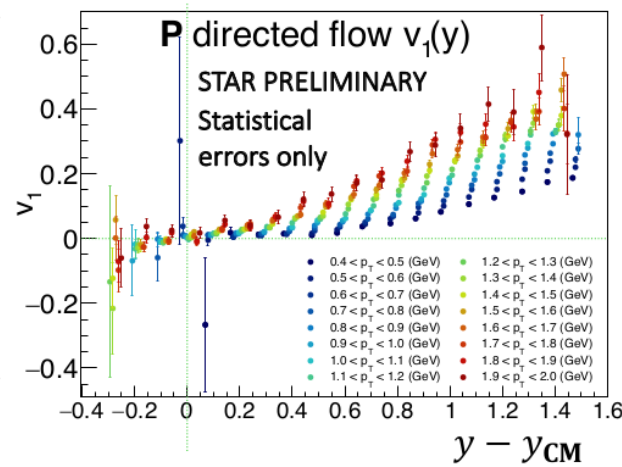
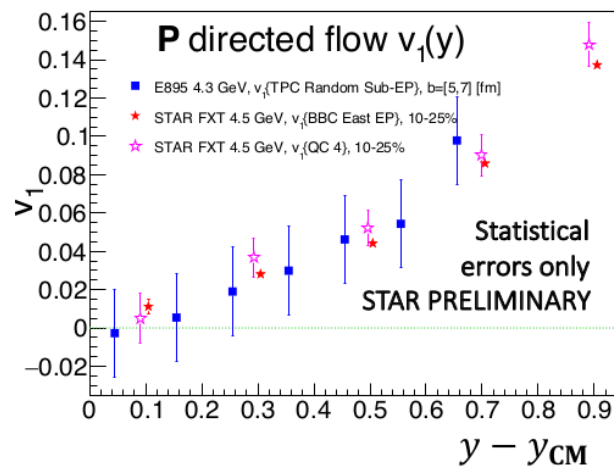
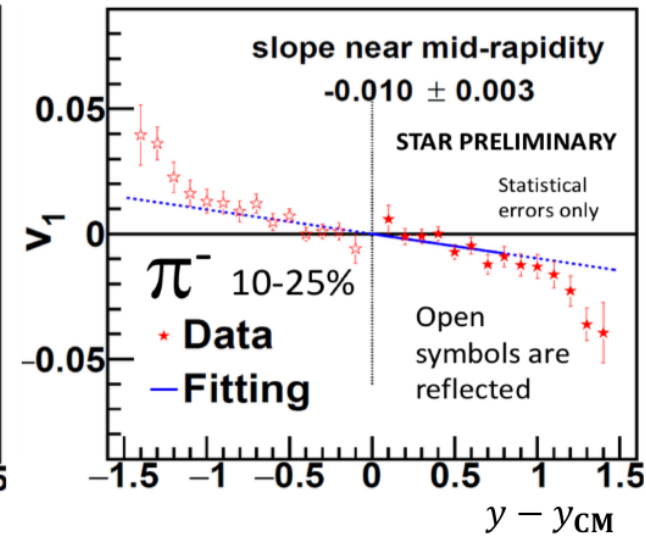
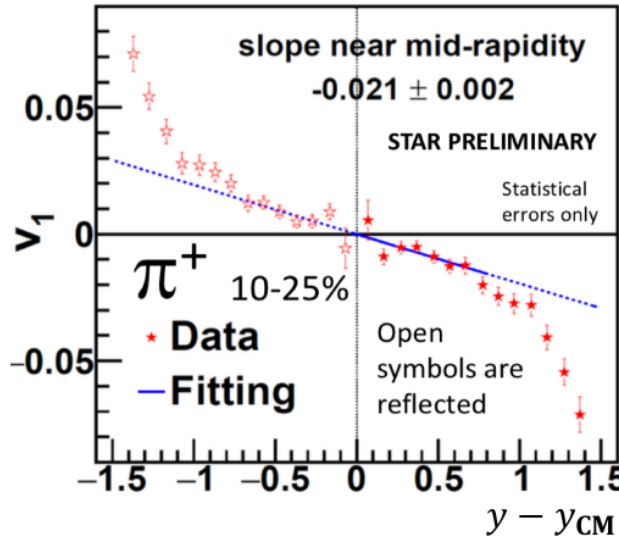
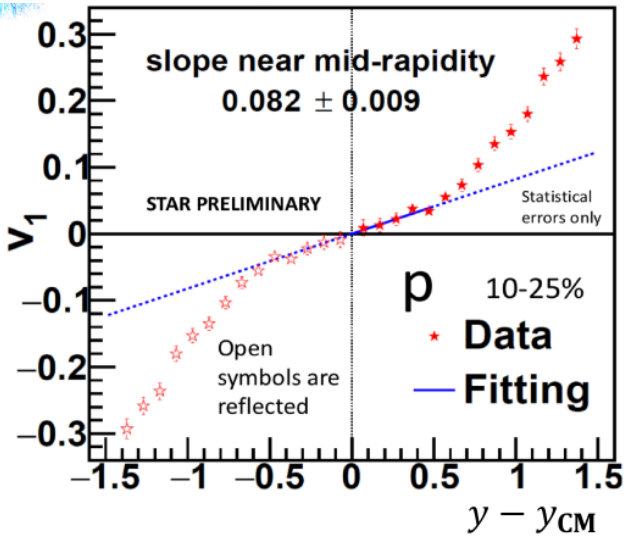


E895 PRC 68 (2003) 054905
 E802 PRC 57 (1998) R466
 E877 PRC 62 (2000) 024901



Negative pion spectra **are consistent** with AGS results.

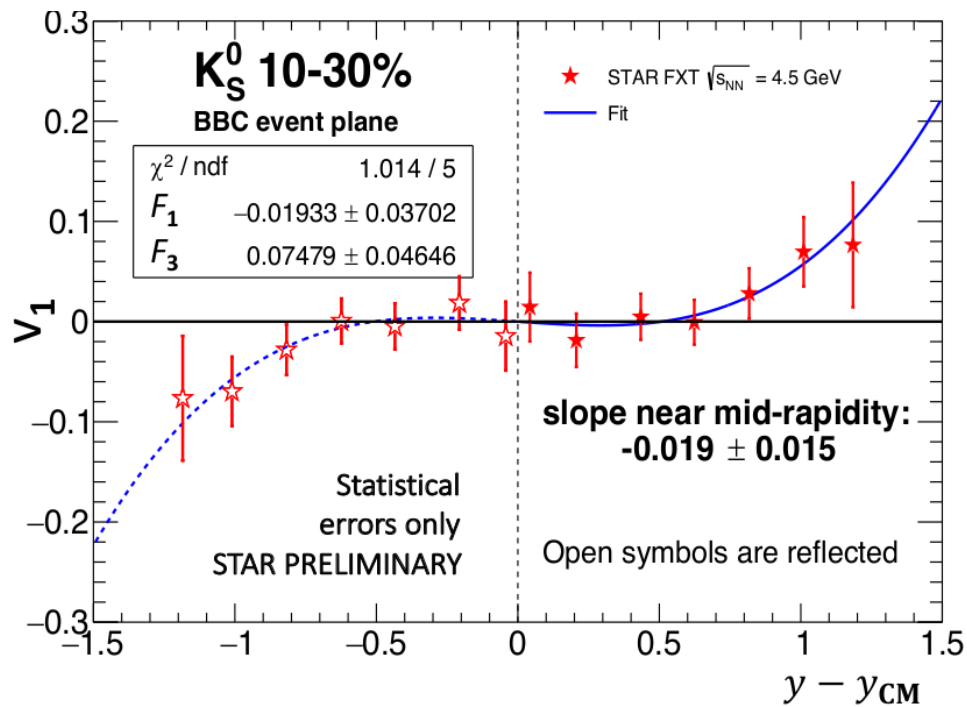
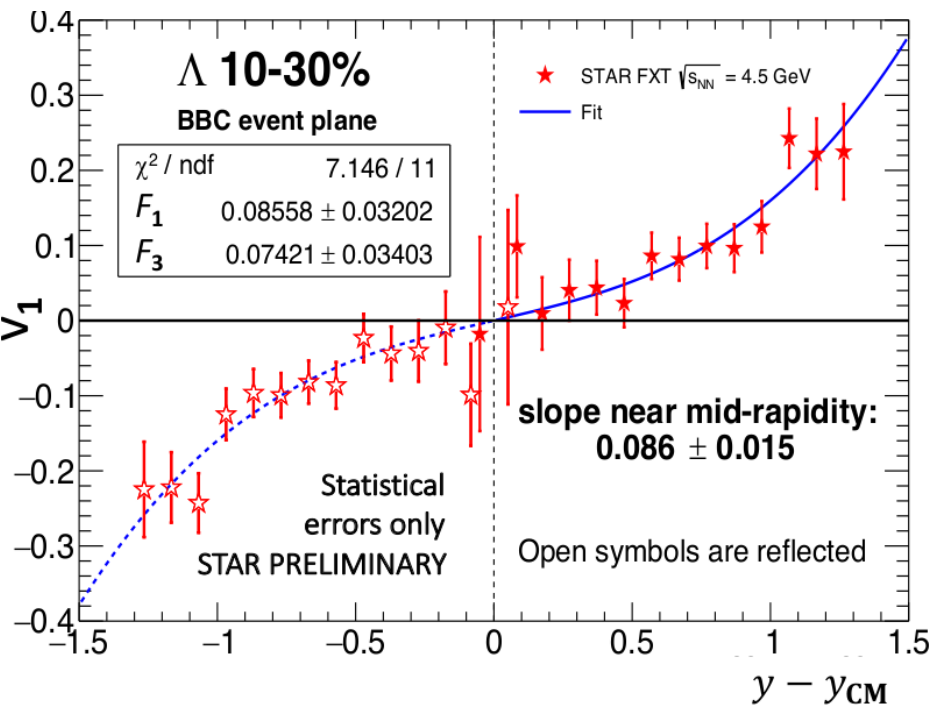
3) Fixed target mode



Directed flow for pions and protons with fit describing mid-rapidity region.

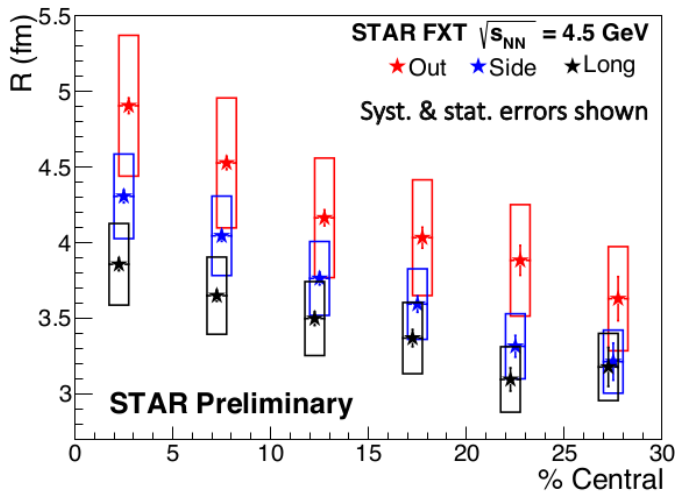
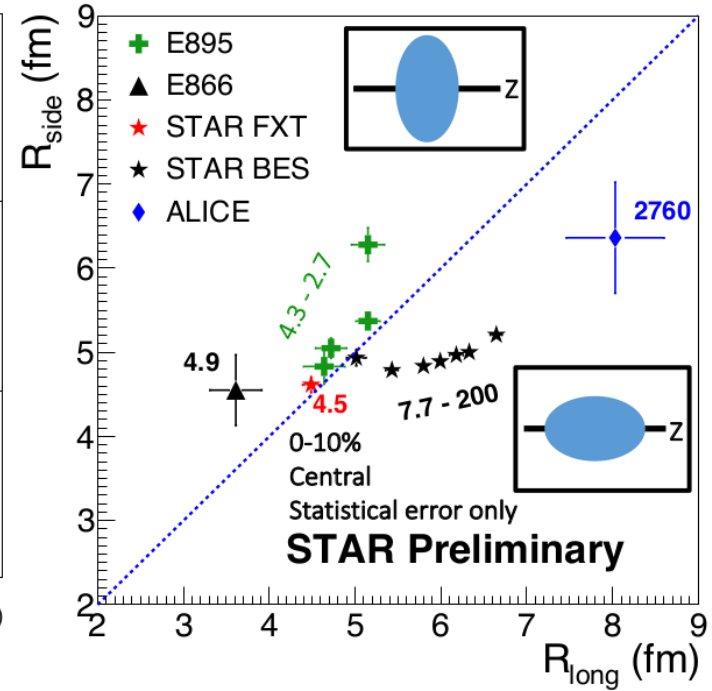
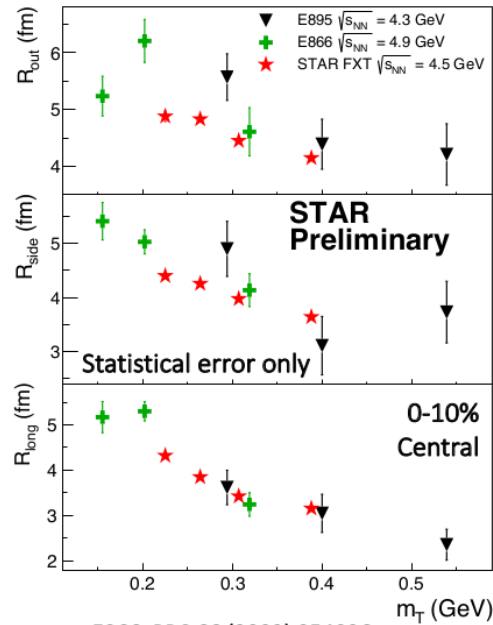
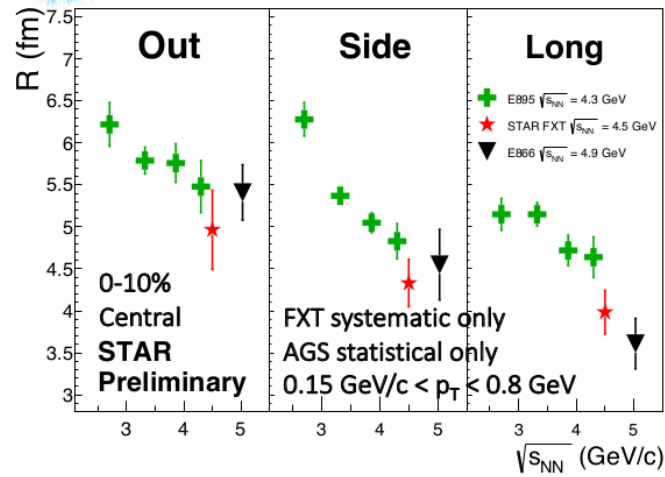
Directed flow of protons **agrees** with AGS results.

3) Fixed target mode



Directed flow for Λ and K_S^0 particles and their fits describing mid-rapidity region.

3) Fixed target mode



E866 PRC 66 (2002) 054096
 E895 PRL 84 (2000) 2798
 ALICE PRB 696 (2011) 328
 STAR PRC 92 (2015) 14904

HBT radii for pions are **consistent** with AGS results.

3) Fixed target mode

- **STAR is ready** to operate with the Fixed Target mode
- **Spectra and particle yields** agree with AGS results
- **Proton directed flow** v_1 agrees with AGS results
- **HBT radii** agree with AGS results

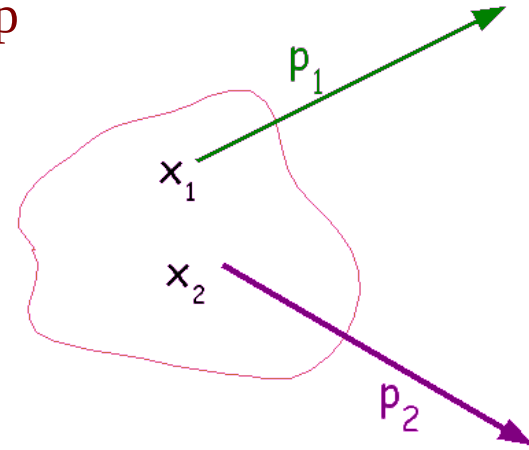
**High-baryon density regime will be accessible with the
Fix Target mode in STAR!**

4) Femtoscopy

Single- and two- particle distributions

$$P_1(p) = E \frac{dN}{d^3 p} = \int d^4 x S(x, p)$$

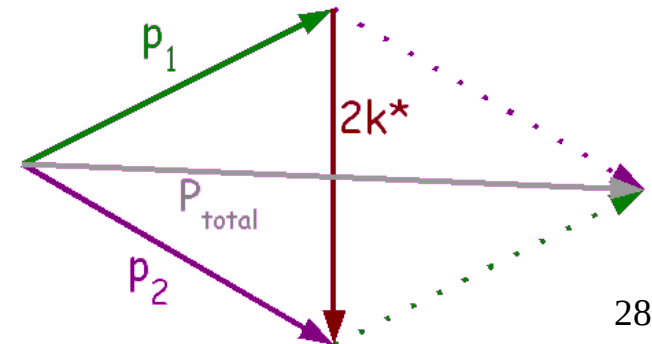
S(x,p) – emission function: the distribution of source density probability of finding particle with x and p



$$P_2(p_1, p_2) = E_1 E_2 \frac{dN}{d^3 p_1 d^3 p_2} = \int d^4 x_1 S(x_1, p_1) d^4 x_2 S(x_2, p_2) \Phi(x_2, p_2 | x_1, p_1)$$

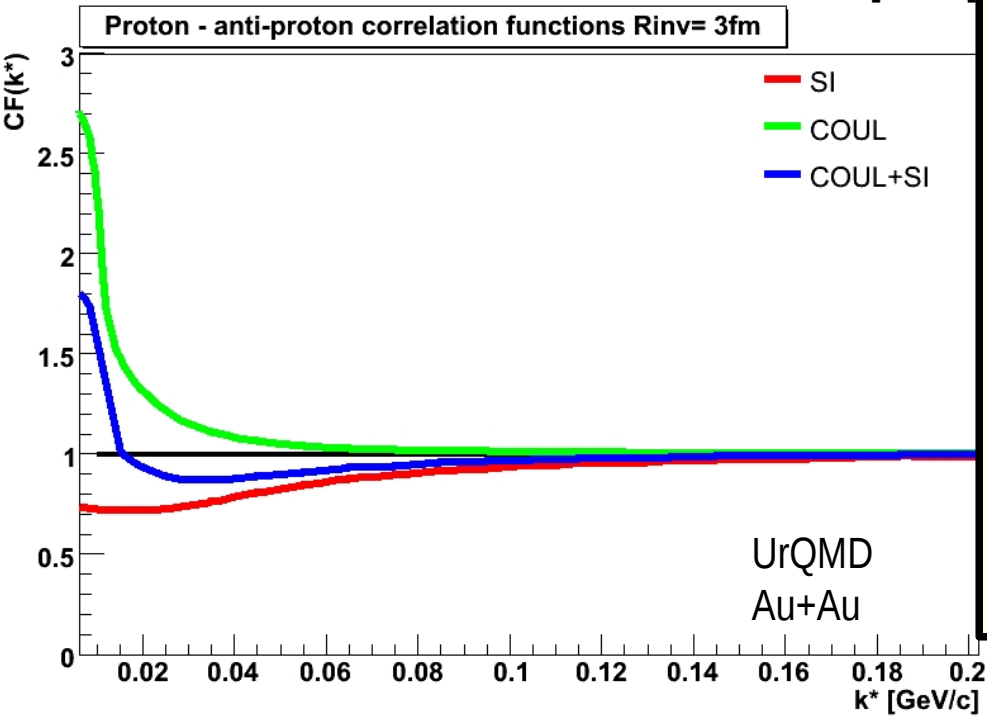
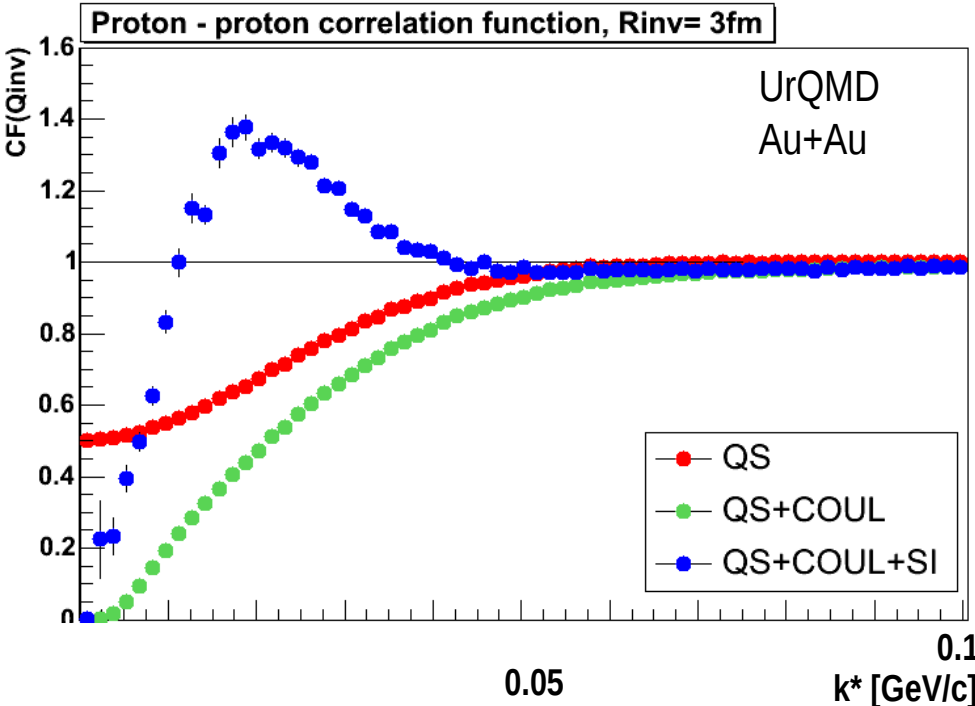
The correlation function

$$C(p_1, p_2) = \frac{P_2(p_1, p_2)}{P_1(p_1) P_1(p_2)}$$



Pair Rest Frame reference

4) Femtoscopy



Identical baryon- baryon

- Quantum Statistics- QS

- Final State Interactions- FSI

- Coulomb

- Strong

Non-identical baryon- (anti)baryon

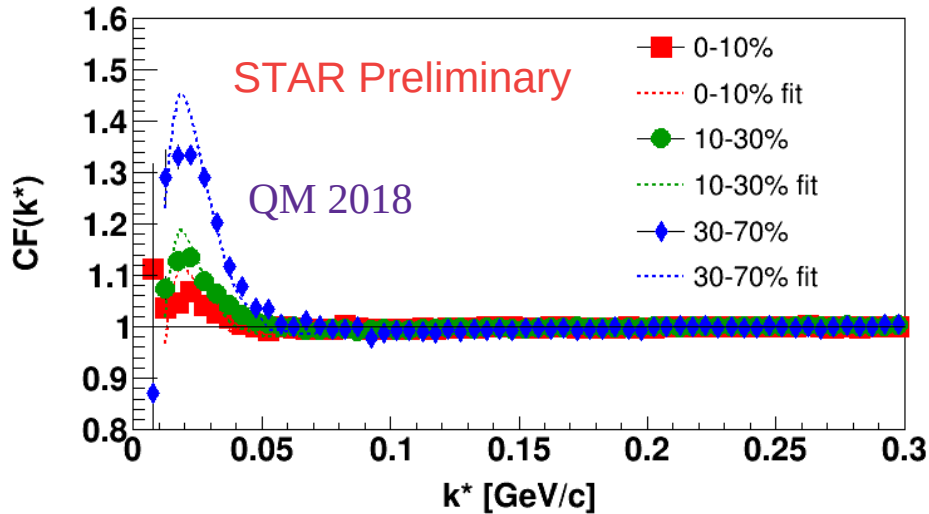
- Final State Interactions- FSI

- Coulomb

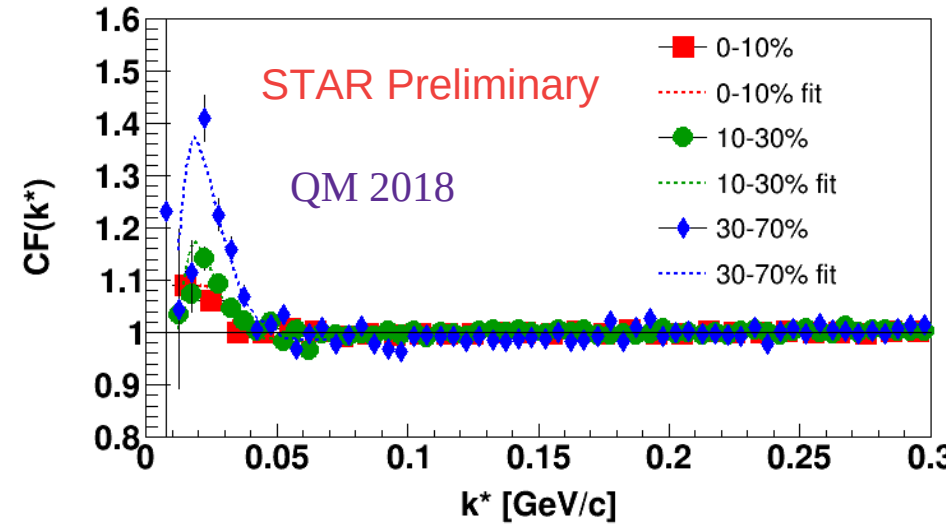
- Strong

4) Femtoscopy

proton-proton @39 GeV



antiproton-antiproton @39 GeV

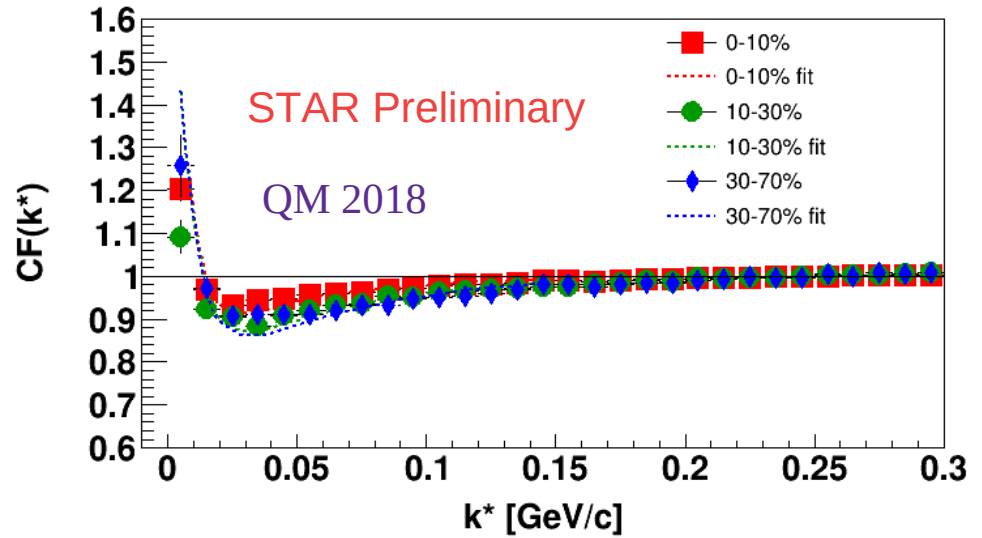


centrality	$R_{inv} p - p$ [fm]	$R_{inv} \bar{p} - \bar{p}$ [fm]	$R_{inv} p - \bar{p}$ [fm]
0-10%	$4.00 \pm 0.15 \pm 0.02$	$3.83 \pm 0.20 \pm 0.03$	$3.39 \pm 0.12 \pm 0.14$
10-30%	$3.61 \pm 0.13 \pm 0.17$	$3.68 \pm 0.15 \pm 0.11$	$2.69 \pm 0.10 \pm 0.12$
30-70%	$2.72 \pm 0.07 \pm 0.07$	$2.95 \pm 0.11 \pm 0.08$	$2.56 \pm 0.09 \pm 0.12$

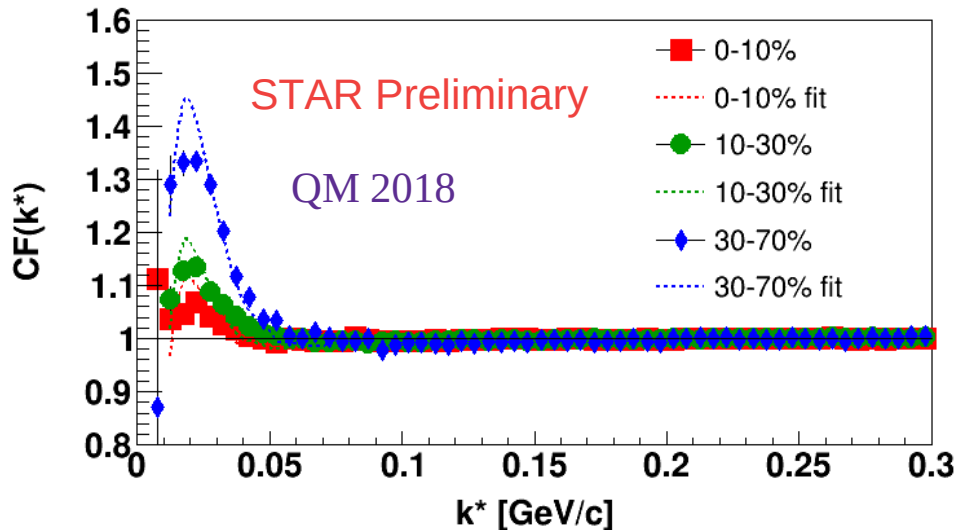
No significant difference between proton-proton and antiproton-antiproton correlation functions

4) Femtoscopy

Radii from proton-proton and antiproton-antiproton systems differ from those from proton-antiproton system →
→ **Residual Correlations.**
Residual feed-down correction needs to be applied.



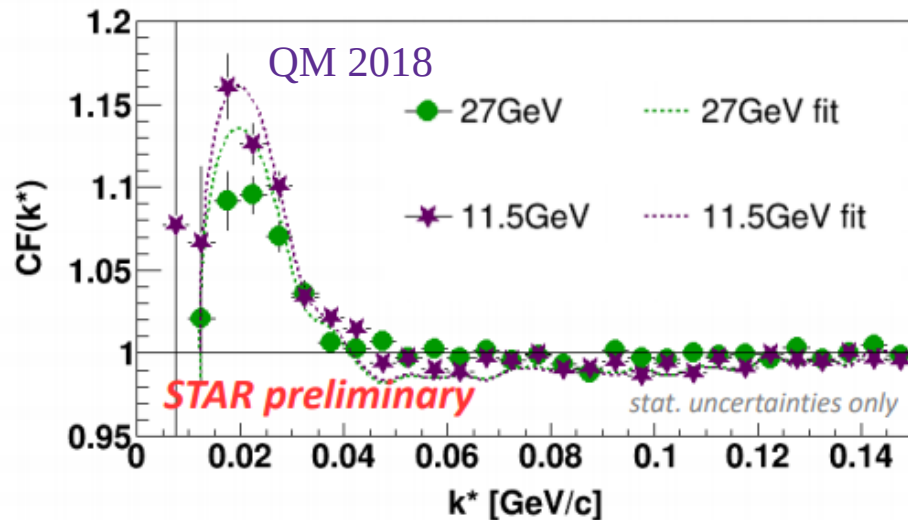
proton-proton @39 GeV



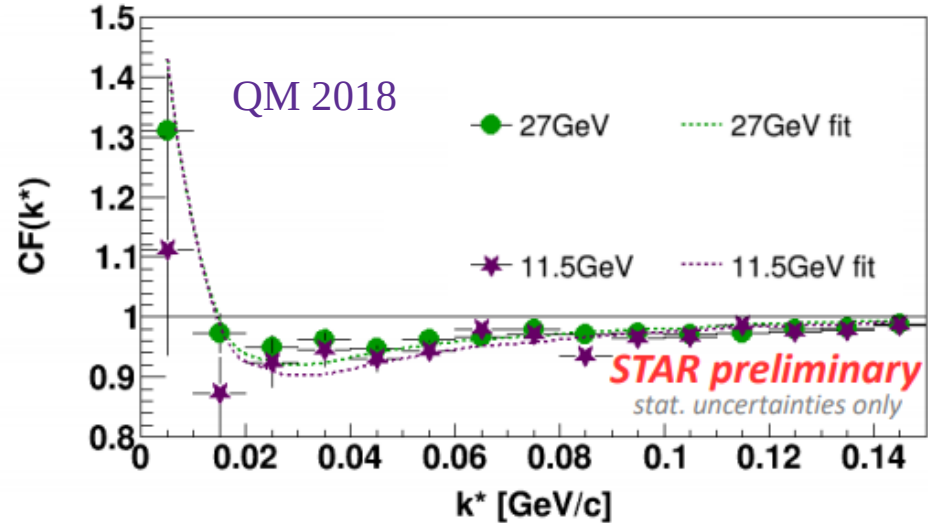
proton-antiproton @39 GeV

4) Femtoscopy

proton-proton, centrality 0-10%



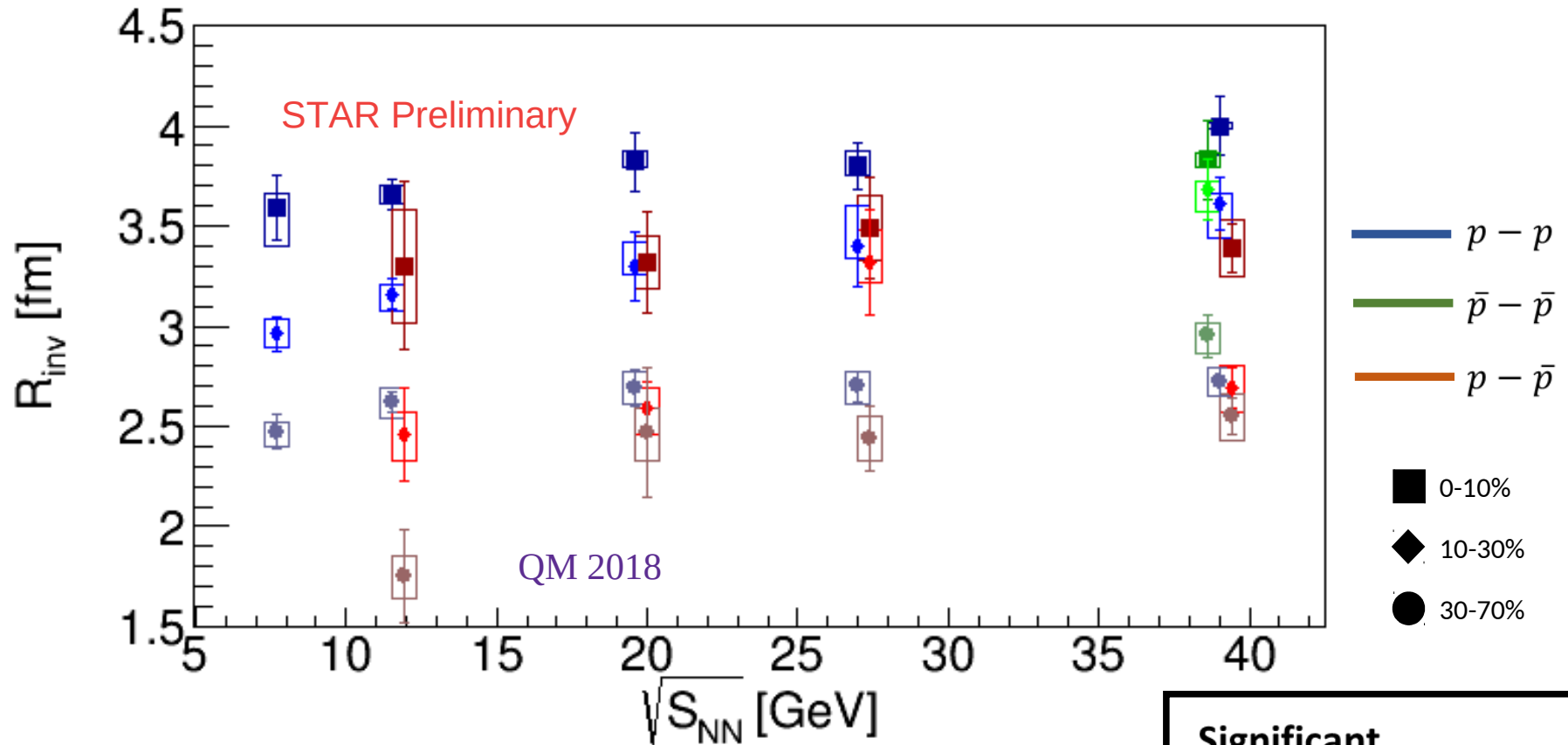
proton-antiproton, centrality 0-10%



energy	$R_{inv} p - p$ [fm]	$R_{inv} p - \bar{p}$ [fm]
7.7 GeV	$3.59 \pm 0.16 \pm 0.19$	
11.5 GeV	$3.66 \pm 0.08 \pm 0.05$	$3.30 \pm 0.42 \pm 0.28$
19.6 GeV	$3.82 \pm 0.15 \pm 0.06$	$3.32 \pm 0.25 \pm 0.13$
27 GeV	$3.80 \pm 0.12 \pm 0.08$	$3.49 \pm 0.25 \pm 0.16$
39 GeV	$4.00 \pm 0.15 \pm 0.02$	$3.39 \pm 0.12 \pm 0.14$

Energy dependence more significant for proton-proton than for proton-antiproton system.

4) Femtoscopy



Feed-down correction may decrease significance of centrality dependence.

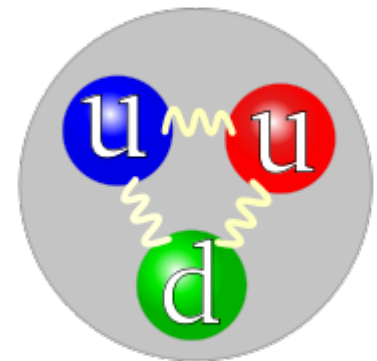
No significant difference between $p - p$ and $\bar{p} - \bar{p}$ correlation functions at $\sqrt{s_{NN}} = 39$ GeV

Significant centrality dependence.

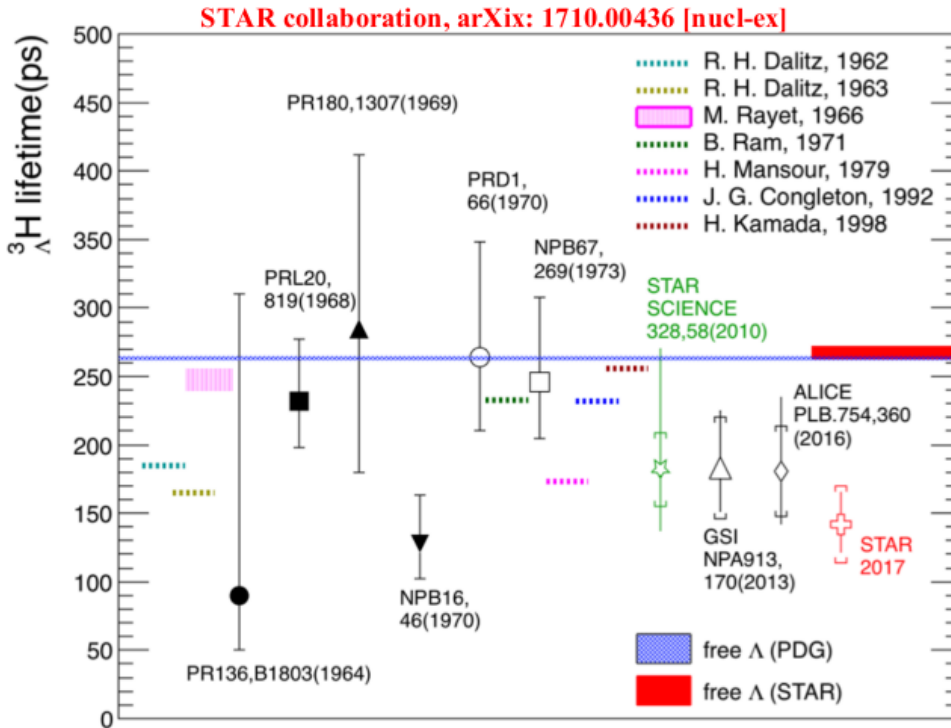
$\sqrt{s_{NN}}$ dependence weak for all centralities.

4) Femtoscopy

- Clear centrality dependence of source size at BES energies
- Visible energy dependence of source size at BES energies
- **No visible difference between proton-proton and antiproton-antiproton correlation functions at $\sqrt{s_{NN}} = 39 \text{ GeV}$**
- **Correlation functions contaminated by residual correlations – residual correction required**



5) Hypertriton

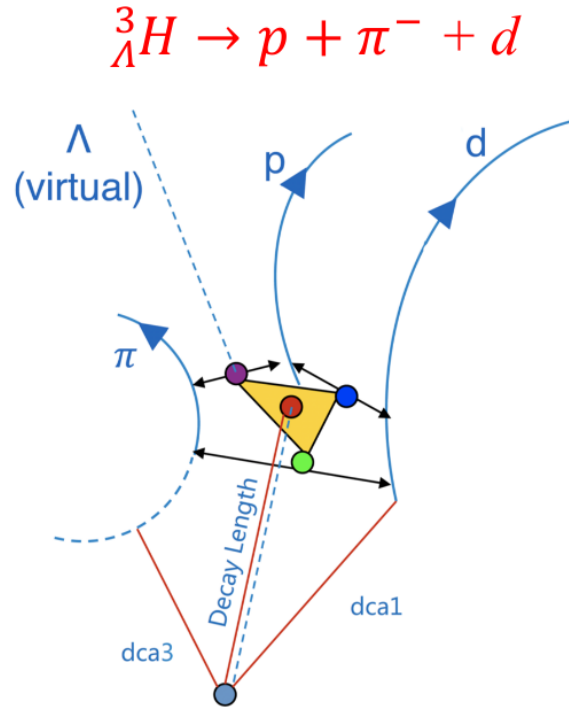
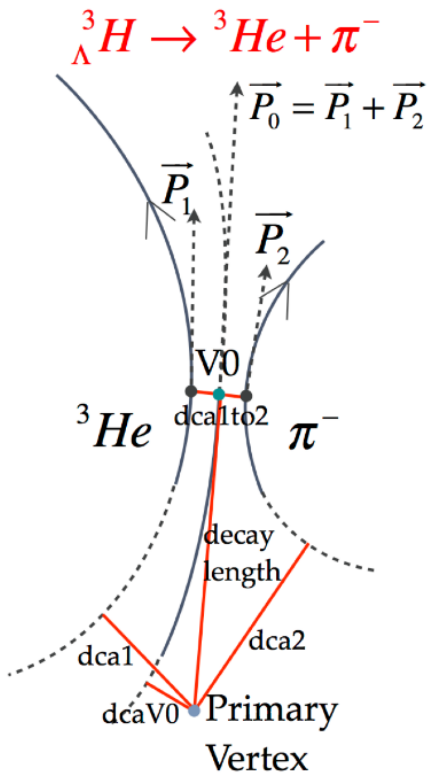


Hyperon-Nucleon:

- play an important role in neutron star and QCD theory
- measurements of masses of hypertriton and anti-hypertriton provide insight into H-N interactions and the CPT symmetry
- measurements sensitive to the temperature and nucleon phase-space of the system freeze-out.
- excellent tool to explore the QCD properties

- [1] R. O. Gomes, V. Dexheimer, S. Schramm, and C. A. Z. Vasconcellos, *The Astrophys. J.* 808, 8 (2015).
- [2] L. L. Lopes and D. P. Menezes, *Phys. Rev. C* 89, 025805 (2014).
- [3] J. Antoniadis et al., *Science* 340, 448 (2013).
- [4] László P. Csernai, Joseph I. Kapusta, *Phys. Repts.* 131, 223 (1986).
- [5] A. Z. Mekjian, *Phys. Rev. C* 17, 1051 (1978).
- [6] Kaijia Sun et al., *Phys. Lett. B* 774, 103 (2017).

5) Hypertriton

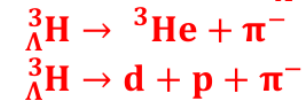


${}^3_{\Lambda}H$ has many decay channels:

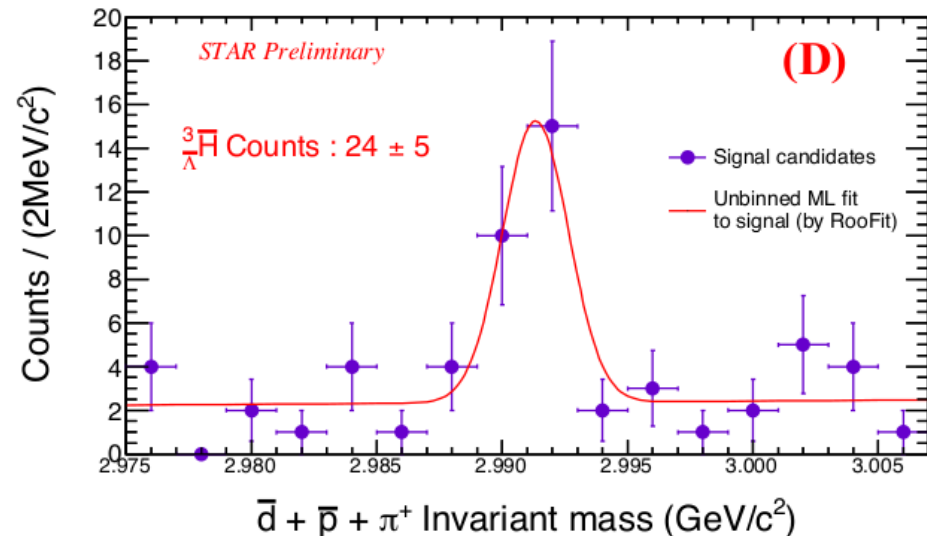
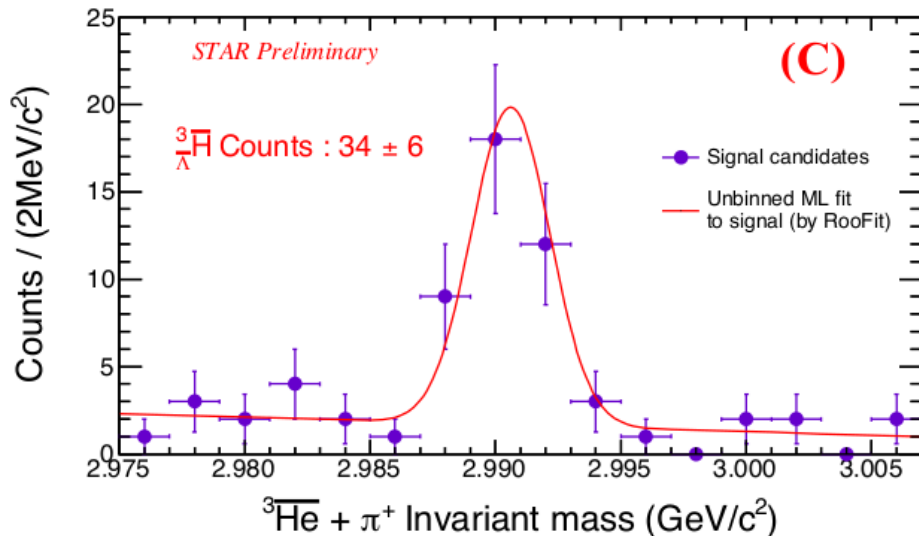
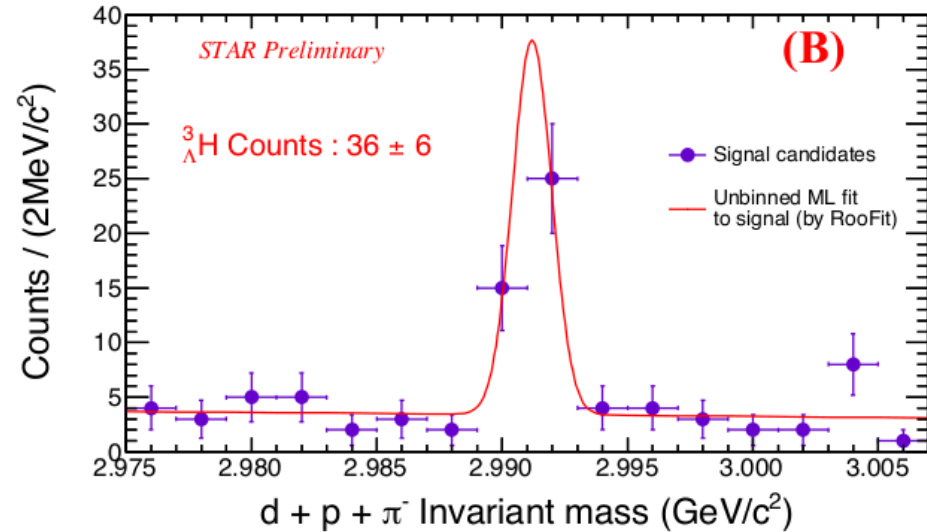
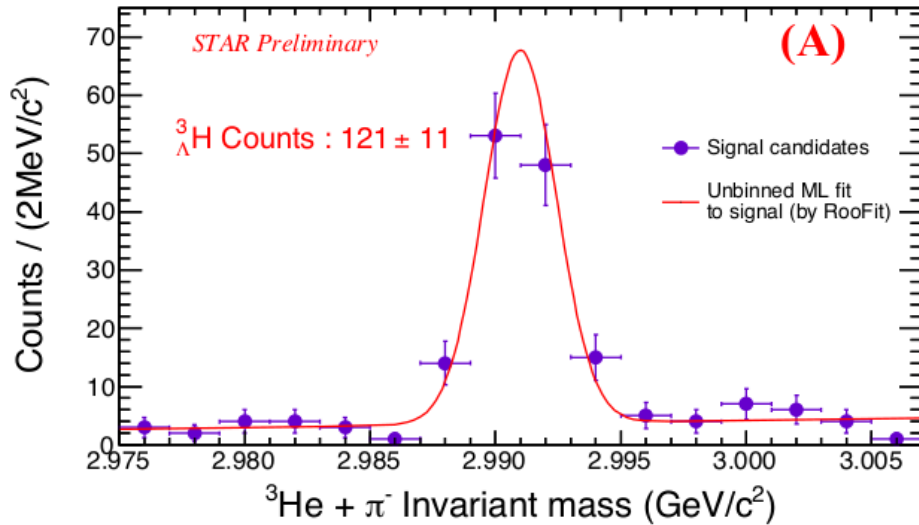
- ✓ Non-meson decay channels:
 - ${}^3_{\Lambda}H \rightarrow d + n$
 - ${}^3_{\Lambda}H \rightarrow p + n + n$
- ✓ Meson decay channels:
 - ${}^3_{\Lambda}H \rightarrow {}^3He$ (3H) + π^{-} (π^0)
 - ${}^3_{\Lambda}H \rightarrow d + p$ (n) + π^{-} (π^0)
 - ${}^3_{\Lambda}H \rightarrow p + n + p$ (n) + π^{-} (π^0)

Good PID of charged particles in STAR detector.

Reconstructing ${}^3_{\Lambda}H$ (${}^3_{\Lambda}\bar{H}$) through:

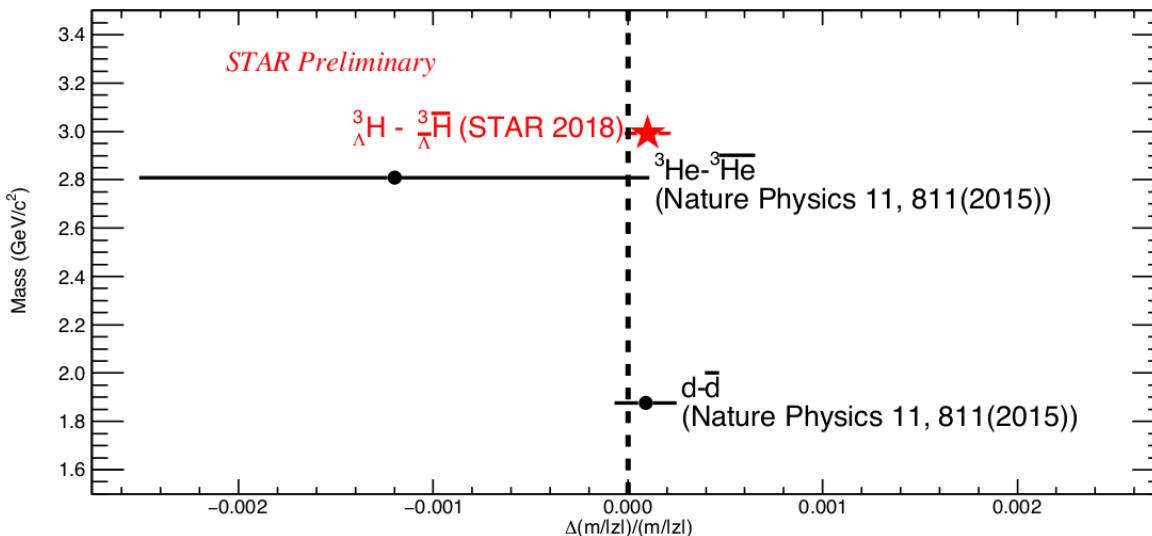
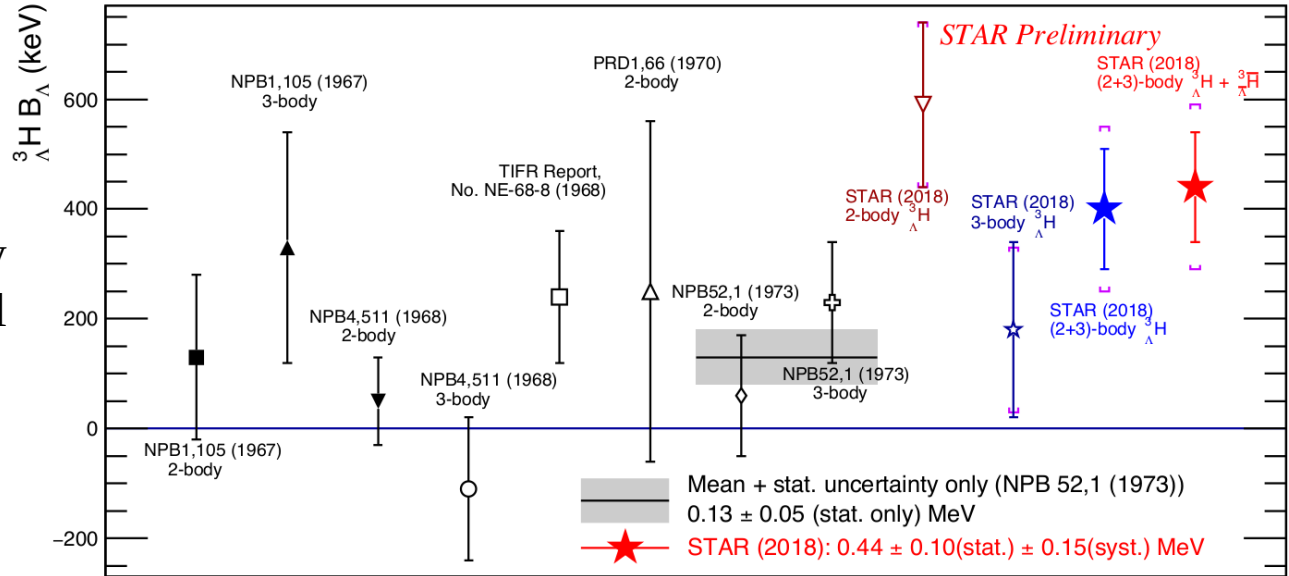


5) Hypertriton



5) Hypertriton

Worldwide binding energy of ${}^3_{\Lambda}\text{H}$ of experimental measurements.



Measurements of the mass-over-charge ratio differences between light nuclei and anti-nuclei.



Conclusions & Summary

Summary

1. **Open heavy flavor** - $D^0 v_1$, $D^0 R_{AA}$ and R_{CP} , Λ_C

2. Quarkonium – ΥR_{AA}

3. Jet modification and high- p_T hadrons - di-jet imbalance, di-hadron correlation

4. Chirality, vorticity and polarization effects - Λ polarization, Φ polarization, CME, CMW

5. **Initial state physics and approach to equilibrium** - v_2 and v_3 fluctuations

6. Collectivity in small systems - v_2 in p+Au and d+Au

7. Collective dynamics - longitudinal decorrelation, identified particle v_1

8. **High baryon density and astrophysics** - v_1 from fixed target

9. **Correlations and fluctuations – femtoscopy**

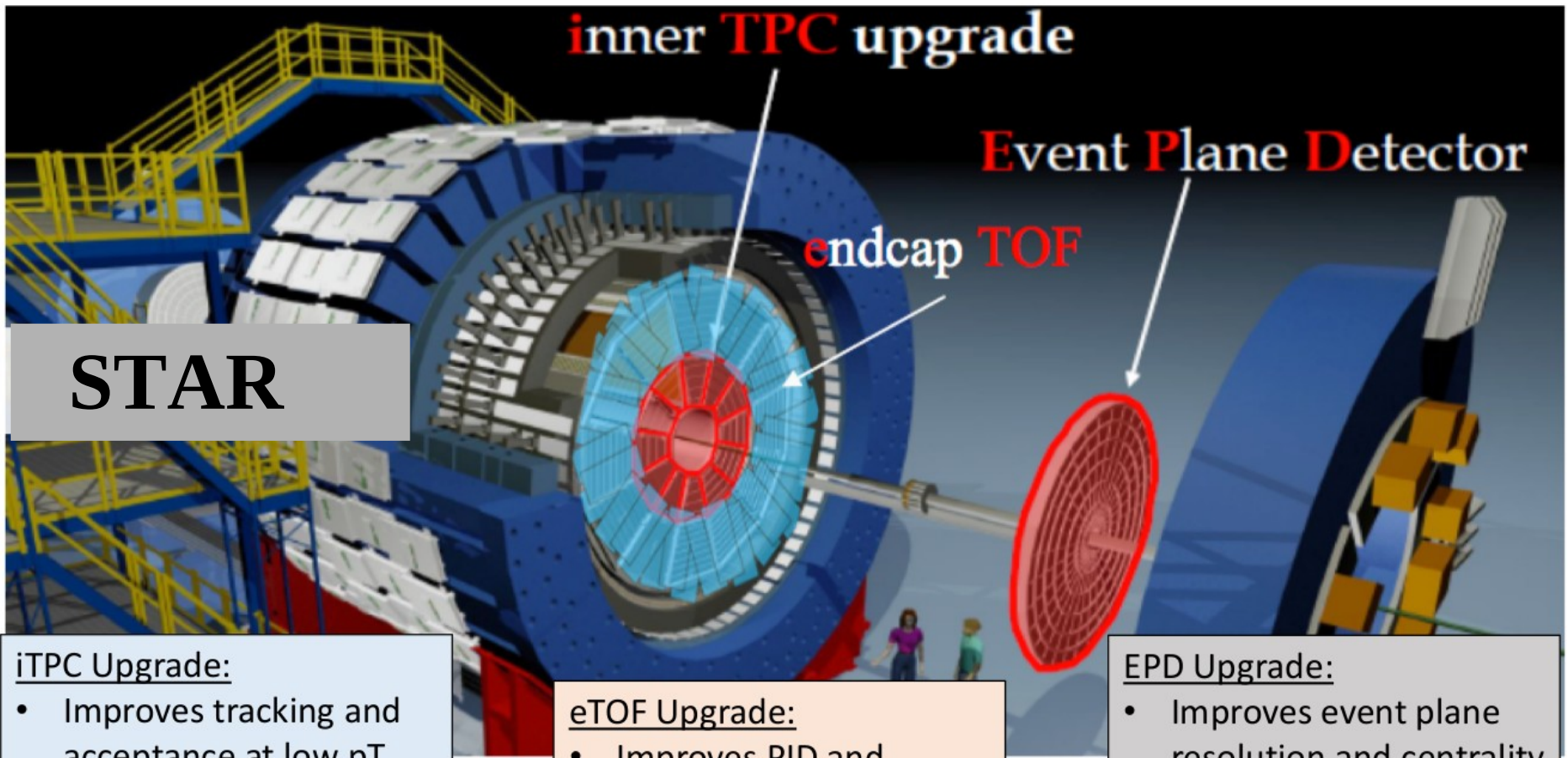
10. **Phase diagram and search for the critical point** - net Λ and off-diagonal cumulants

11. **Thermodynamics and hadron chemistry** - triton, hypertriton mass

12. **Upgrades** - BES-II and forward upgrades



Upgrades



STAR

iTPC Upgrade:

- Improves tracking and acceptance at low p_T and extra y acceptance
- Ready in 2019

eTOF Upgrade:

- Improves PID and acceptance
- Ready in 2019

EPD Upgrade:

- Improves event plane resolution and centrality definition
- Taking data in 2018 run

STAR Note 0644: Technical Design Report for the iTPC Upgrade

arXiv:1609.05102v1 [nucl-ex]

STAR Note 0666: An Event Plane Detector for STAR

Upgrades

STAR Note 0696: STAR Collaboration Beam Use Request for Run 19+ (Scenario 1)

Single Beam Energy (GeV/nucleon)	$\sqrt{s_{NN}}$ (GeV)	Run Year	Run Time	Species	Min-Bias Events Number
5.75	3.5 (FXT)	2020	2 days	Au+Au	100M
7.3	3.9 (FXT)	2019	2 days	Au+Au	100M
9.8	4.5 (FXT)	2019	2 days	Au+Au	100M
13.5	5.2 (FXT)	2020	2 days	Au+Au	100M
19.5	6.2 (FXT)	2020	2 days	Au+Au	100M
31.2	7.7 (FXT)	2019	2 days	Au+Au	100M

- ❖ iTPC & eTOF upgrades will be available
- ❖ Need 100M events at each energy to match sensitivity of BES-II: 2 days per energy (3.5 GeV – 7.7 GeV)
- ❖ Data rate is DAQ limited
- ❖ Data at 7.7 GeV will provide an overlap energy with collider mode

FXT in Run 18

Trigger commissioning occurring now

1 Billion events at 7.2 GeV

100 Million events at 3.0 GeV

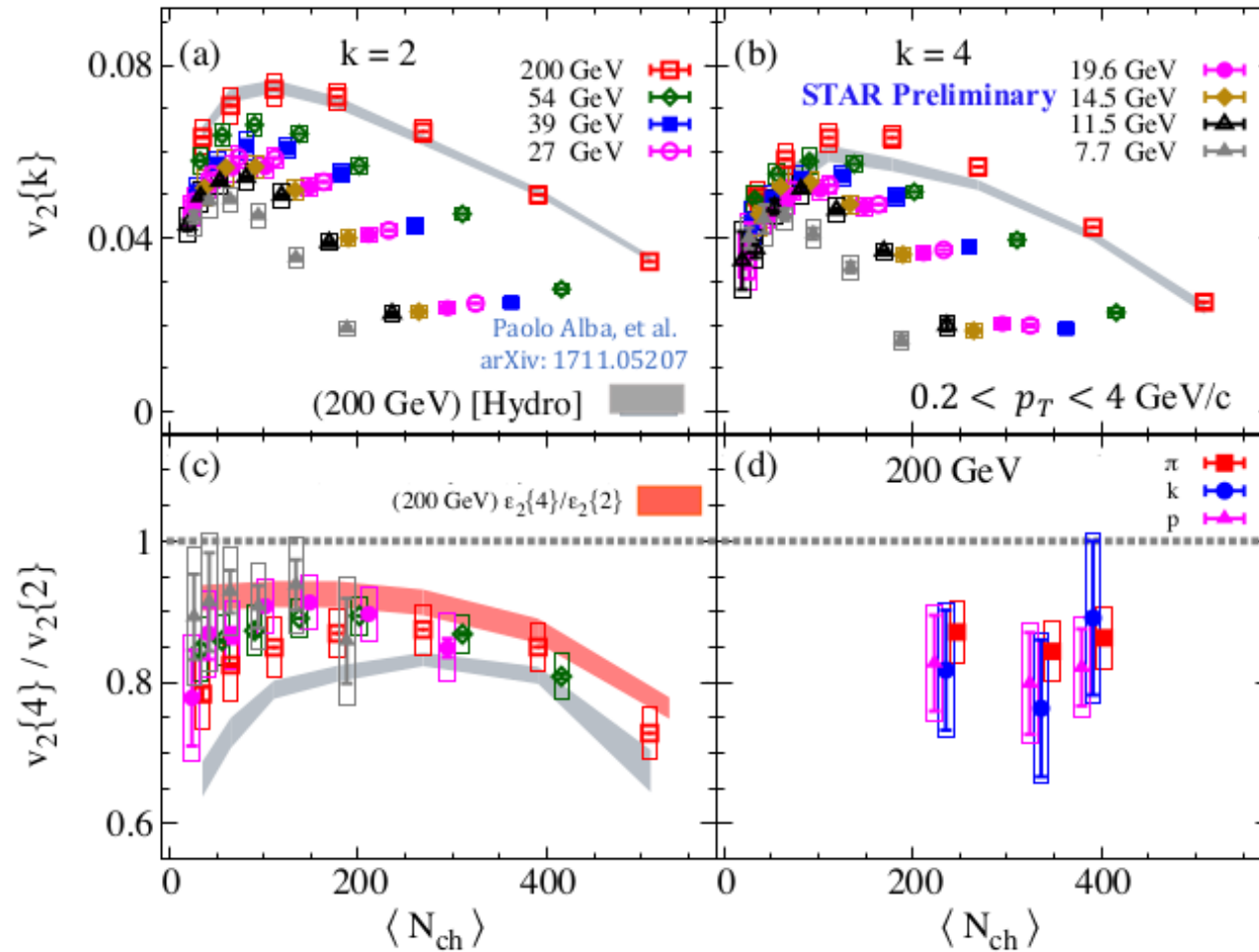
EPD ready and available for flow analyses

Can obtain fluctuation measurement at energies below BES-I

Thank you!

Backup slides

2) Initial state physics

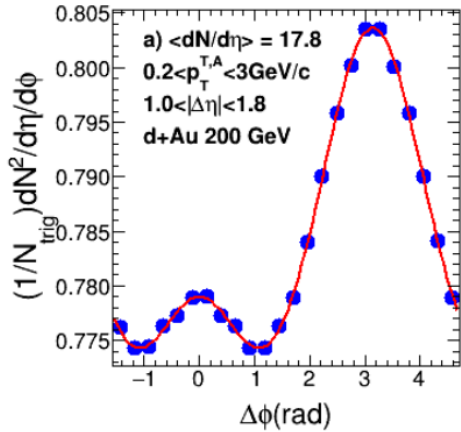


Strong dependence on collision energy

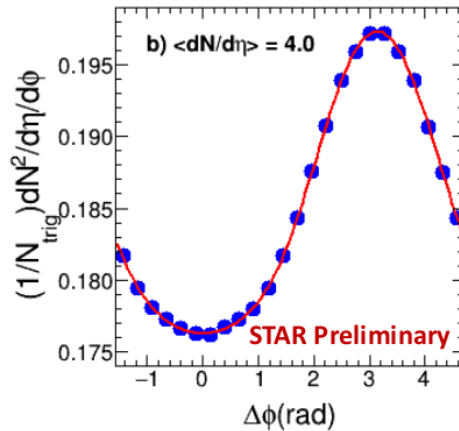
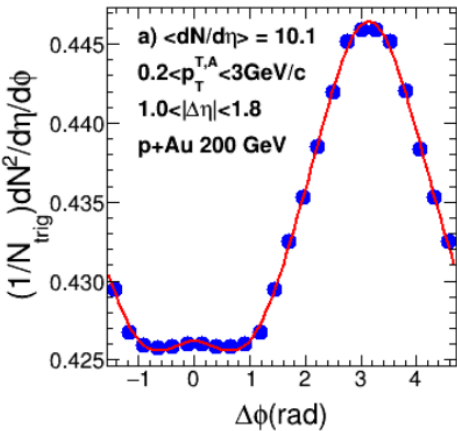
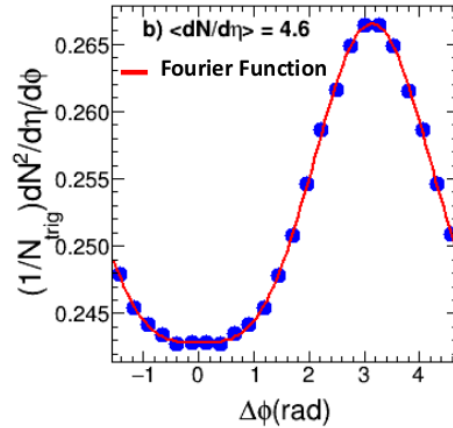
Weak dependence on collision centrality

3) Small systems

High Multiplicity (HM)



Low Multiplicity (LM)



d+Au 200 GeV High Multiplicity (HM) of d+Au collisions

p+Au 200 GeV

$$dN/d\Delta\phi \sim 1 + \sum_{n=1}^4 2V_{n,n} \times \cos(n\Delta\phi)$$

$$\text{Integral } v_n = \text{sqrt}(V_{n,n}); v_n(p_T) = V_{n,n}(p_T)/v_n$$

3) Small systems

Low multiplicity subtraction scaled by short-range near-side ($|\Delta\eta| < 0.5$) jet yield

$$V_{n,n}^{HM}(\text{subtracted}) = V_{n,n}^{HM} - V_{n,n}^{LM} \times \frac{N_{asso}^{LM}}{N_{asso}^{HM}} \times \frac{Y_{jet,near-side}^{HM}}{Y_{jet,near-side}^{LM}}$$

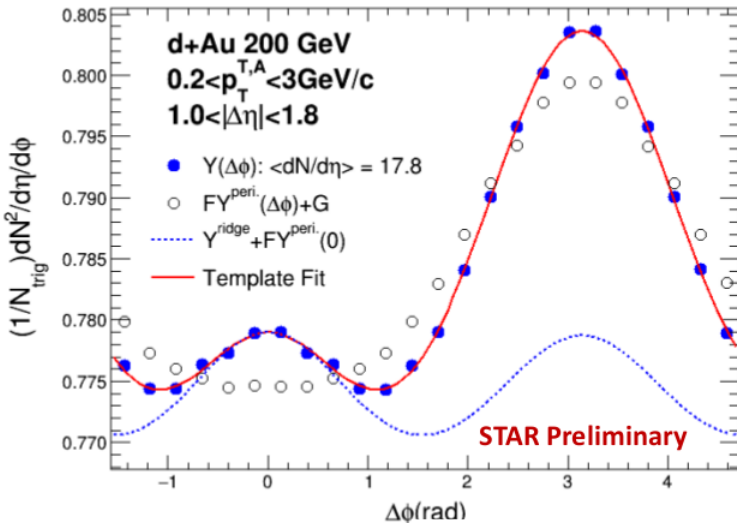
ATLAS:PRC90(2014)044906

CMS:PLB765(2017)193

STAR: PLB743(2015)333

Short-range near-side jet modification = long-range away-side jet modification

Template fit



$$Y_{templ.}(\Delta\phi) = F \times Y_{LM}(\Delta\phi) + Y_{ridge}(\Delta\phi)$$

where

$$Y_{ridge}(\Delta\phi) = G \times (1 + 2 \times \sum_{n=2}^4 V_{n,n} \times \cos(n\Delta\phi))$$

ATLAS:PRL(116)172301

A new method by ATLAS Collaboration away-side jet shape can be measured in Low Multiplicity (LM) events scaled by "F" parameter (due to jet modification)

3) Small systems

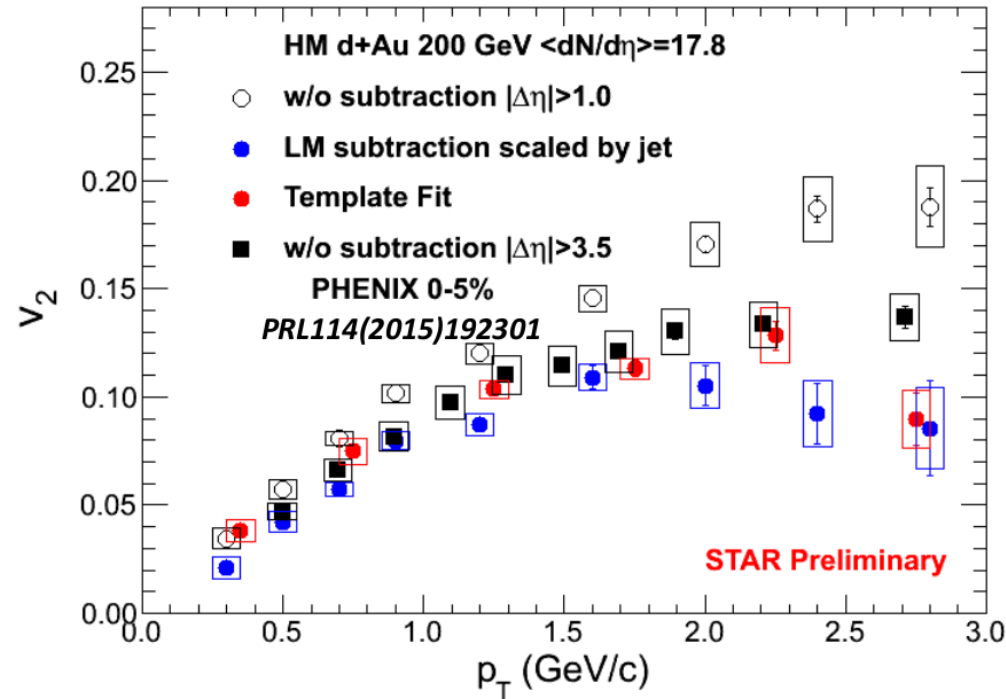
v_2 without subtraction is **larger** than that with subtraction for both methods.

The subtraction of non-flow contributions are very **important** for STAR results are comparable with PHENIX results, except at high p_T .

At lowest p_T v_2 from Low Multiplicity subtraction is **35% lower** than from template fit

At intermediate p_T they **agree** with each other

STAR results are **comparable** with PHENIX ones.

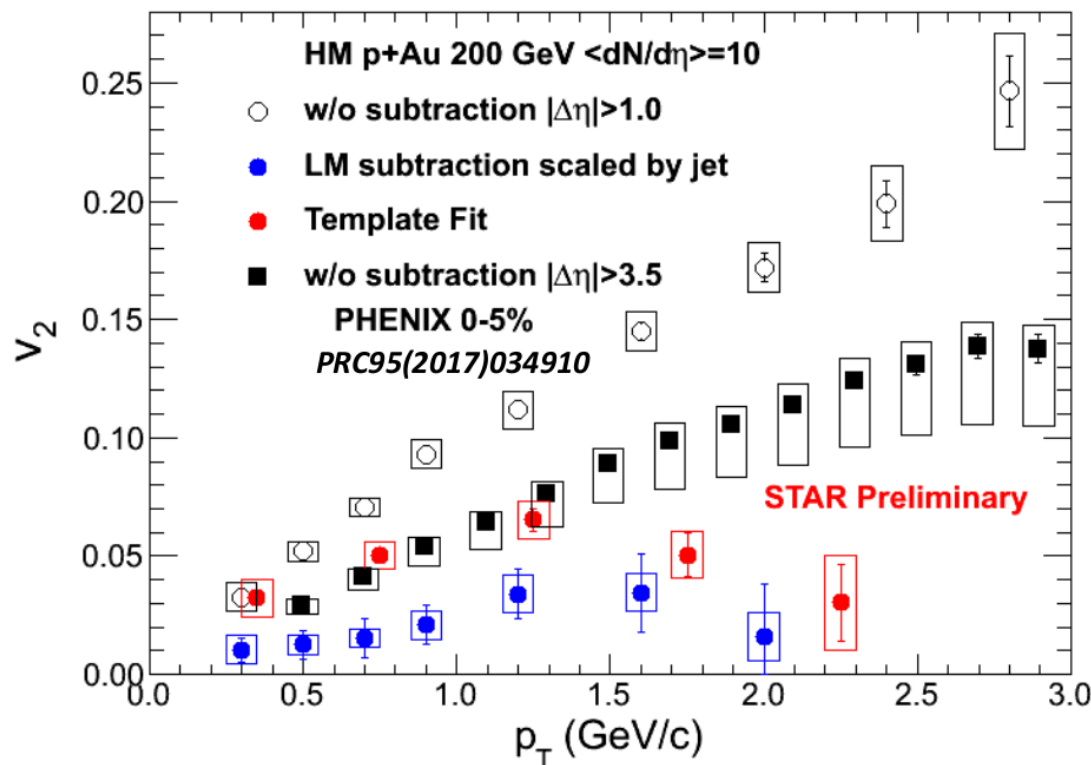


3) Small systems

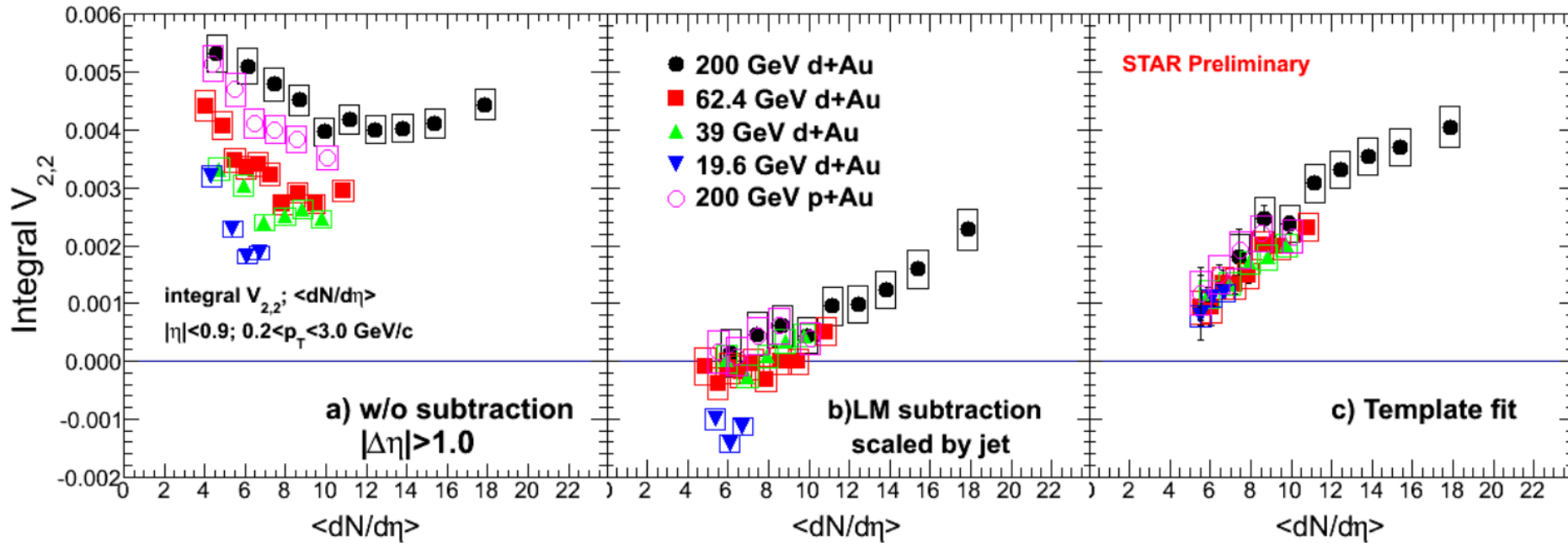
v_2 in p+Au collisions without subtraction is **larger** than v_2 in d+Au collisions that with subtraction for both methods.

v_2 in p+Au collisions from Low Multiplicity subtraction is **lower** than from template fit.

STAR results are **comparable** with PHENIX results, except at high p_T . The STAR data is clearly lower than PHENIX for $p_T > 1.5$ GeV/c



3) Small systems



Large **difference** between subtraction method and template fit

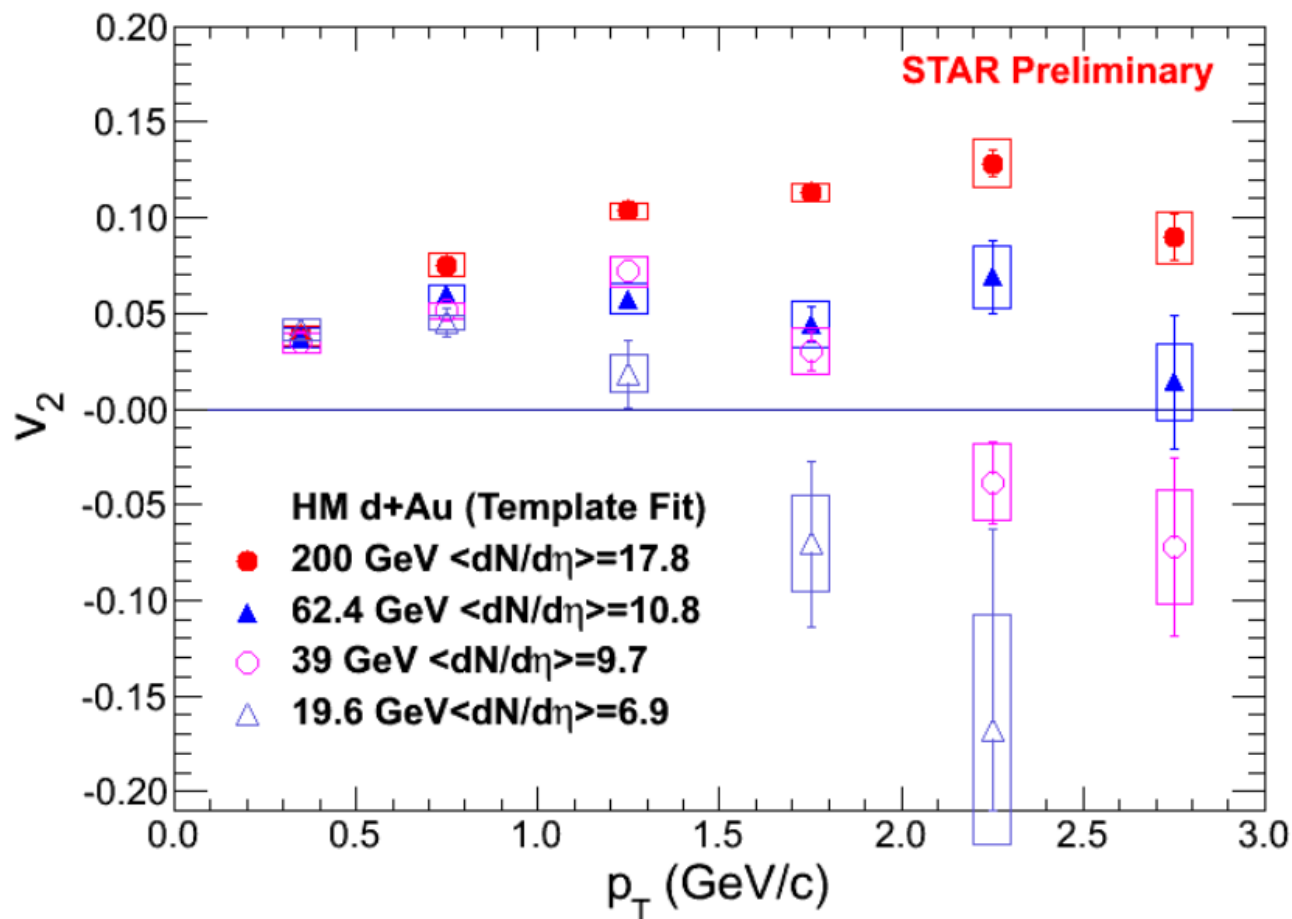
v_2 from subtraction method is **negative** at lower collision energies (different kinematics between near-side and away-side jet-like correlations?)

v_2 from template fit **increases** with collision centrality

3) Small systems

v_2 becomes **negative** at high transverse momentum in d+Au collisions at low collision energy

The correlation from away-side jet is **stronger** at high transverse momentum



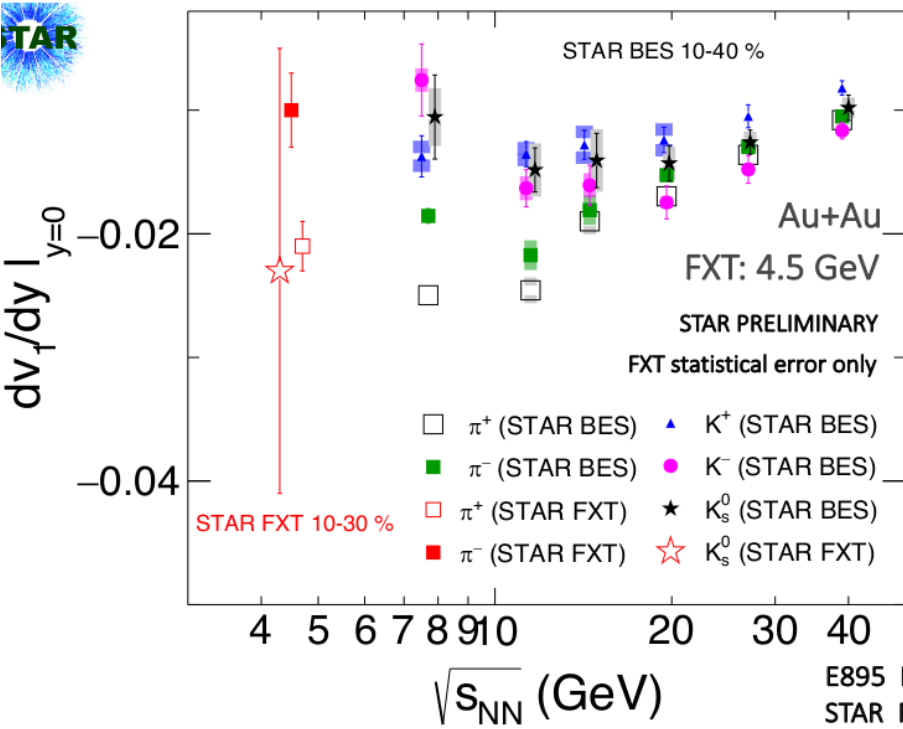
3) Small systems

Large **difference** between v_2 from two methods has been observed at low energy \rightarrow large uncertainties in the non-flow subtraction in small systems.

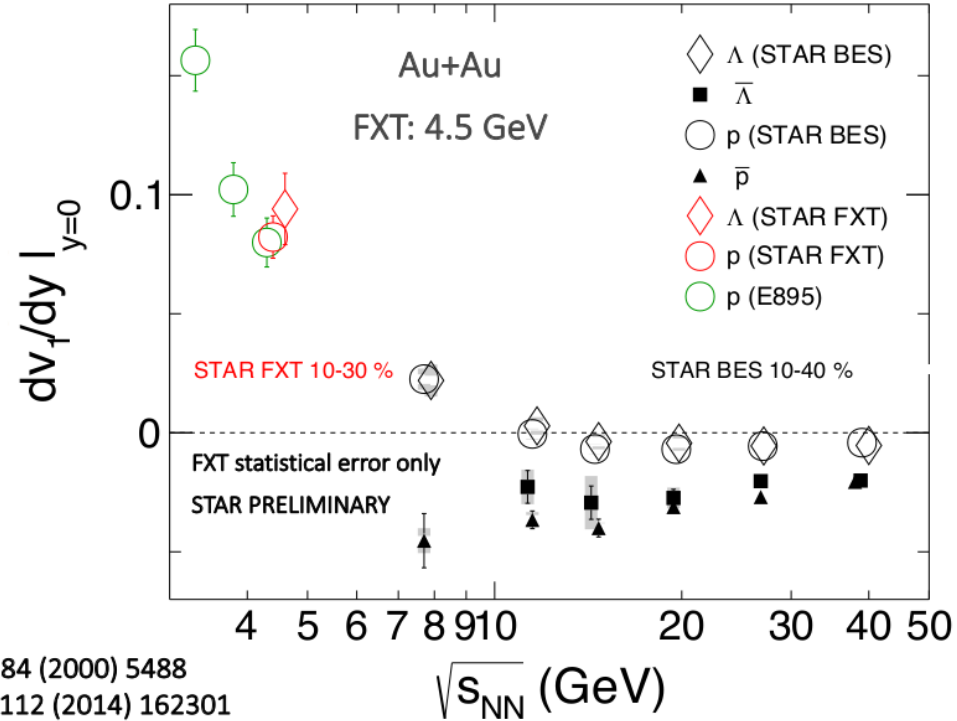
We do see **similar** v_2 between p+Au and d+Au collisions for same multiplicity $\rightarrow v_2$ is not only driven by initial geometry.

The integral v_2 extracted by a template fit shows an **universal** trend as a function of $\langle dN/d\eta \rangle$ for different small systems at different energies \rightarrow multiplicity plays an important role in small systems.

3) Fixed target mode



E895 PRL 84 (2000) 5488
STAR PRL 112 (2014) 162301



Directed flow for identified particles **agrees** with AGS results.

6) Hipertriton

Triton from Au+Au Collision

